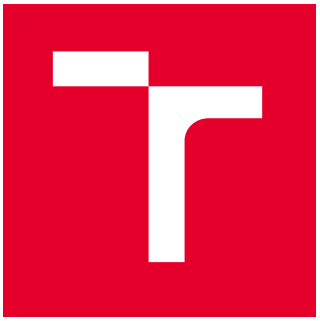

BRNO UNIVERSITY OF TECHNOLOGY

VYSOKÉ UČENÍ TECHNICKÉ V BRNĚ

FACULTY OF ELECTRICAL ENGINEERING AND COMMUNICATION

FAKULTA ELEKTROTECHNIKY
A KOMUNIKAČNÍCH TECHNOLOGIÍ

DEPARTMENT OF RADIO ELECTRONICS

ÚSTAV RADIOELEKTRONIKY

EDUCATIONAL NANOSATELLITE IN POCKETQUBE FORMAT

VÝUKOVÝ NANOSATELIT FORMÁTU POCKETQUBE

MASTER'S THESIS
DIPLOMOVÁ PRÁCE

AUTHOR — **Bc. Jakub Lokaj**
AUTOR PRÁCE

SUPERVISOR — **Ing. Aleš Povalač, Ph.D.**
VEDOUCÍ PRÁCE

BRNO 2023

BRNO UNIVERSITY OF TECHNOLOGY
FACULTY OF ELECTRICAL ENGINEERING AND COMMUNICATION

Master's Thesis

Master's study program **Electronics and Communication Technologies**

Department of Radio Electronics

Student: Bc. Jakub Lokaj ***ID:*** 203515

Year of study: 2 ***Academic year:*** 2022/23

TITLE OF THESIS:

Educational Nanosatellite in PocketQube Format

RECOMMENDED LITERATURE:

[1] KASAL, Miroslav. Směrové a družicové spoje: přednášky. Vyd. 2. V Brně: Vysoké učení technické, Fakulta elektrotechniky a komunikačních technologií, Ústav radioelektroniky, 2003. ISBN 80-214-2496-6.

[2] CAPPELLETTI, Chantal, Simone BATTISTINI a Benjamin MALPHRUS. CubeSat Handbook: From Mission Design to Operations. 1. ed. London: Academic Press, 2020. ISBN 978-0-12-817884-3.

Date of project specification: 6.2.2023 ***Deadline for submission:*** 22.5.2023

Supervisor: Ing. Aleš Povalač, Ph.D.

doc. Ing. Lucie Hudcová, Ph.D.
Chair of study program board

Abstract

The main topic of this diploma thesis was the theoretical analysis of current trends in the development of nanosatellites, specifically focusing on the PocketQube format and its actual implementation. In the individual theoretical chapters, it is discussed the possibilities and advantages of using PocketQube as a learning model for educational and developmental fields. There are explored 3D printing options for the supporting structure of the satellite and discuss individual components such as the on-board computer, communication system based on LoRa, power system, and an overview of subsystems. In the practical part, there were developed the frame of the satellite, individual parts of the PocketQube electronics structure, and implemented the basic functionality of communication and operation for the educational PocketQube model.

Keywords

PocketQube, LoRa communication, STM32, 3D print, EPS, OBC

Abstrakt

Hlavním tématem této diplomové práce byla teoretická analýza současných trendů ve vývoji nanosatelitů, konkrétně se zaměřením na formát PocketQube a jeho aktuální implementaci. V jednotlivých teoretických kapitolách se práce zabývá možnostmi a výhodami využití PocketQube jako výukového modelu pro vzdělávací a vývojové oblasti. Zabývá se také možnostmi 3D tisku nosné konstrukce družice a rozebírám jednotlivé komponenty, jako je palubní počítač, komunikační systém založený na technologii LoRa, napájecí systém a přehled subsystémů. V praktické části byl vyvinut rám družice, jednotlivé části struktury elektroniky PocketQube a implementace základní funkce komunikace a provozu pro vzdělávací model PocketQube.

Klíčová slova

PocketQube, komunikace LoRa, STM32, 3D tisk, EPS, OBC

Bibliographic citation

LOKAJ, Jakub. Educational nanosatellite in PocketQube format. Brno: Brno University of Technology, Faculty of electrical engineering and communications, Dept. of telecommunications, 2021. 83 p., 10 p. of attachments. Master's thesis. Advised by Ing. Aleš Povalač, Ph.D.

Author’s Declaration

Author:	*Jakub Lokaj*
Author’s ID:	*203515*
Paper type:	*Master’s Thesis*
Academic year:	*2022/23*
Topic:	*Educational Nanosatellite in PocketQube Format*

I declare that I have written this paper independently, under the guidance of the advisor and using exclusively the technical references and other sources of information cited in the project and listed in the comprehensive bibliography at the end of the project.

As the author, I furthermore declare that, with respect to the creation of this paper, I have not infringed any copyright or violated anyone’s personal and/or ownership rights. In this context, I am fully aware of the consequences of breaking Regulation S 11 of the Copyright Act No. 121/2000 Coll. of the Czech Republic, as amended, and of any breach of rights related to intellectual property or introduced within amendments to relevant Acts such as the Intellectual Property Act or the Criminal Code, Act No. 40/2009 Coll., Section 2, Head VI, Part 4.

.

Brno, June 6, 2023 ----------

author’s signature

Acknowledgement

I would like to express my sincere gratitude to my advisor, Aleš Povalač, for his invaluable assistance with resolving issues throughout my project. His expertise and guidance have been instrumental in overcoming technical challenges and ensuring the smooth progress of my work.

Brno, June 6th, 2023 ----------

Author's signature

Contents

FIGURES

TABLES

1. INTRODUCTION

Satellite development was once a domain exclusive to government agencies in its early stages. However, as technology progressed, the development of satellites began to shrink in size thanks to the advancements in microelectronics. This led to the creation of CubeSats, which have been gaining popularity in recent years due to their low overall development cost and low launch costs. CubeSats are standardized small satellites, with sizes ranging from 10cm x 10cm x 10cm for 1U, 1.5U, 2U, 3U CubeSats. The opportunities presented by CubeSats have opened doors for small companies, as well as universities and students. The first CubeSat was introduced in a publication from California State Polytechnic University in 1999, and since then, the development of these small satellites has progressed significantly. [1]

However, the need for smaller satellites persisted, leading to the development of the PocketQube satellite. These satellites measure only 5cm x 5cm x 5cm in size, making them a miniature version of the already small CubeSats, with a maximum weight of 250 grams. The affordability and availability of microprocessors have been instrumental in the development of PocketQubes, which offer a range of benefits. Not only are they suitable for a specific payload, but their size also affects the equipment inside the satellite. At first, it was believed that eight PocketQubes could fit inside a single CubeSat deployer in a 2x2x2 configuration, but further research yielded a separate deployer for PocketQubes, known as MRFOD.

The first PocketQube was presented in a paper by Prof. Bob Twiggs in 2009, and since then, the development of PocketQubes has continued. [4] The smaller size of these satellites allows for more flexibility in launch options and deployment methods. This makes them particularly suitable for academic research projects, where they offer a low-cost alternative to larger and more expensive satellites. In conclusion, the development of CubeSats and PocketQubes has revolutionized the satellite industry, making it more accessible to small companies and academic institutions. The affordability and ease of development of these small satellites have led to a new era of space exploration and research, opening up endless possibilities for innovation and discovery. [1] [2] [3]

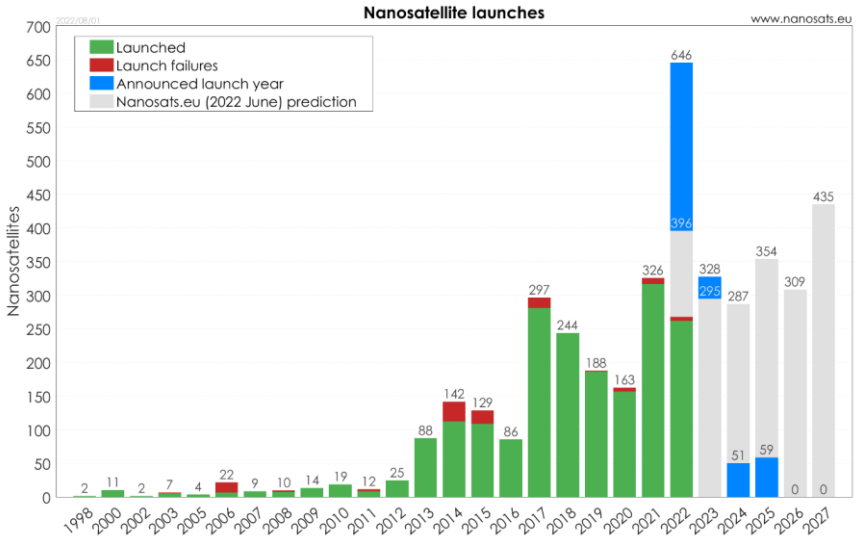

Figure 1: Statistics of released nanosatellites [28]

1.1 Potentional applications for the PocketQubes

1.1.1 For educational purposes

Practical hands-on experience on real devices can always motivate and offer a better understanding compared to theoretical education. PocketQubes, as a small satellite platform, provide an opportunity for students to comprehend the fundamentals of satellites. There is still room for development and the design of new technologies, and the miniaturization of systems presents new challenges for university students.

The concept of educational nanosatellites is to provide students with a hands-on experience of what it takes to develop such satellites. In the long run, the intention is to expose students to the complete development process in iterations, including the design of individual subsystems or components of the satellite. This exposure will enable them to use these skills directly in the space industry and in their future professional roles.

The aim is for students to gain practical experience in building, testing, and operating PocketQubes. This practical experience will provide a more profound and comprehensive understanding of the challenges and opportunities involved in developing and deploying such small satellites. The ultimate goal is to prepare students for a career in the space industry, where they can apply the skills and knowledge they gained from their hands-on experience.

Moreover, the educational value of PocketQubes extends beyond the space industry. The skills learned during the development of these small satellites can be applied in various other industries and fields. This includes but is not limited to, robotics, communications, and remote sensing.

In summary, the use of PocketQubes as an educational tool provides an opportunity for students to acquire practical skills and hands-on experience in satellite development.

This experience can lead to a better understanding of the challenges and opportunities in the space industry and prepare students for their future careers. Additionally, the skills gained from the development of PocketQubes have practical applications in other fields and industries as well. [3]

1.1.2 Demonstration of new technologies and innovations

PocketQube, being a low-cost platform, presents an opportunity to test and demonstrate new technologies in space. By miniaturizing subsystems of larger satellite platforms, PocketQube can serve as a means to showcase new technologies such as solar sensors, which can be tailored to its size. However, it is hard to note that technical parameters must be significantly reduced as only the technology under test would be the payload. Therefore, testing on orbit would prove challenging to verify if PocketQube is capable of providing reference measurements with sufficient quality.In addition to subsystem demonstrations, PocketQube also holds potential for future applications, such as using a constellation of 10 to 60 units to test platform-independent algorithms for new communication techniques like IoT. This setup could provide high coverage of the planet without the need for communicating with large satellites during specific time windows.

Another area of interest is demonstrating the use of blockchain technology for securing communication between satellites. Furthermore, PocketQube could serve as a platform to test distributed systems like flight in formation or docking.Another potential application for PocketQube is the demonstration of new materials that can measure thermal resistance, known as "thermal payload". The use of new optical reflectors or theoretical radar calibration experiments can also be tested on this platform. The versatility and low-cost of PocketQube allow for a wide range of possibilities for new technologies and their demonstrations. [3] [7]

1.1.3 Observation of the Earth, Sun and Stars

The observation of the Earth, Sun, and stars is a important aspect of modern space exploration. CubeSats, such as those with a size of up to 6U [5], are commonly used for Earth observation, while PocketQubes like the CShark Pilot-1 2P Earth Observation and IoT Satellite from FOSSA Systems are also being employed in this field. These miniature satellites test new technologies and techniques, such as low-power communication and miniaturized optical systems for remote sensing. However, due to the limitations of their size, PocketQubes are not as suitable for observation purposes as CubeSats. One of the challenges with PocketQubes is the Ground Sampling Distance (GSD), which is typically twice as small as that of larger CubeSats. Nonetheless, the development of new technologies and the growing interest in space-based observation continues to drive innovation in this field. [6]

1.2 Orbit for PocketQube

In general, almost all the satellites that travel in space are typically placed in a Low Earth Orbit (LEO) zone, which is usually within the range of 400-800 kilometers, but can be as far out as 2000 kilometers. The satellite's orbital period is typically around 90-93 minutes, meaning that when tracking it in orbit, we can only see it for approximately 10-15 minutes at a time, and usually only about 2-3 times during its overall pass, or approximately 15.5-15.9 times per day (24 hours). Each orbit is shifted westward by approximately 22.9 degrees. There are two commonly used orbits that have almost zero eccentricity, or are minimally elliptical (almost circular), with a perigee and apogee (nearest and furthest point) that are almost the same. The velocity of the orbit is approximately 7.8 kilometers per second.

The most commonly used orbits are the two mentioned above, one with an altitude of 300-500 kilometers and an inclination of 51.6 degrees, known as the International Space Station (ISS) orbit. The second is at an altitude of 500-800 kilometers with an inclination of 98 degrees, known as the Sun-Synchronous Orbit (SSO), which means it has a fixed position relative to the Sun. This orbit has a slightly tilted rotation plane with a deviation of 20 to 30 degrees. The advantage of this orbit is that the satellite always passes over the same spot at local time. It is worth noting that there are many other types of orbits that can be used for different purposes, depending on the specific mission requirements.. [7]

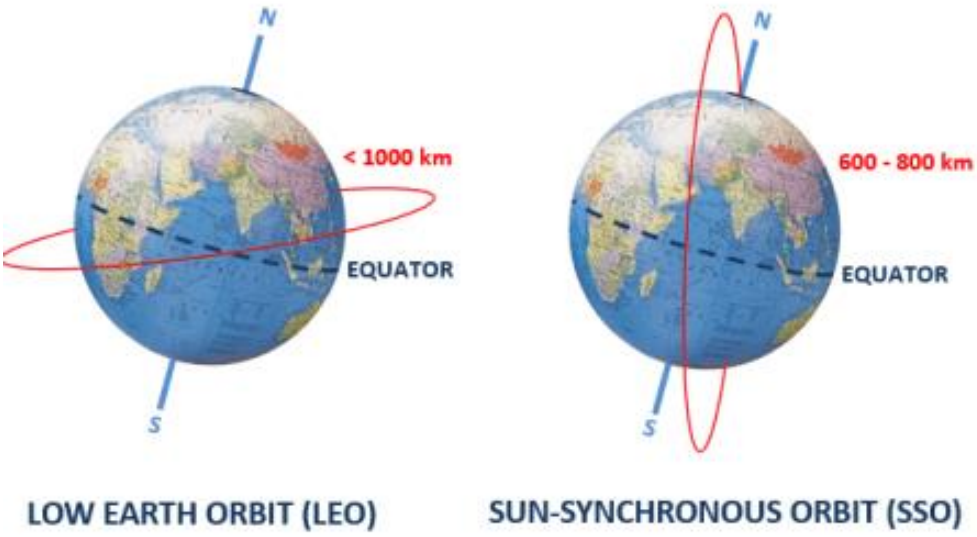

Figure 2: Illustration of Earth orbits [2]

1.3 PocketQube Deployer

A deployment module, which is commonly used to launch satellites into space, is a main element in the launching process. The module typically uses a spring mechanism to push the satellites into orbit through an opening door. The deployment device itself remains attached to the launch vehicle. Within the deployer, the satellites are usually slid and carefully placed into the designated holes or rails. The cost of launching a Cubesat satellite into space can be quite expensive, often ranging from $100,000 to $300,000. However, the smaller PocketQube satellites offer a more affordable alternative with a cost range of around $25,000. This is why many universities and research institutions are particularly interested in this type of satellite. [2]

One of the well-known commercial deployers available for PocketQube satellites is provided by AlbaOrbital. The AlbaPod (as shown in Figure 3) is specifically designed to deploy satellites that meet certain regulations, such as a weight limit of 250 grams for 1p (500 grams for 2p, 750 grams for 3p). Additionally, all satellites must have a redundant switch that connects the satellite's batteries to the electronics. This means they must be discharged at the AlbaPod (deployers) itself. In accordance with PQ-Mech-12, a minimum of 2 kill switches (SPDT roller limit switch - e.g. OMROM D2F-L2-A-ND) are required for each satellite. These switches should be located under the bottom of the satellite within 20mm on the front of the Z+ or Z-. Furthermore, specific requirements such as the material used for the base plate (FR4, anodized or allochromatic aluminum) and qualification tests (vibration test for sinusoidal and random vibration) must be met. [11]

Figure 3: AlbaPod PocketQube deployer [29]

Besides AlbaOrbital, there are several manufacturers that produce deployers specifically designed for PocketQube satellites. One of these companies is Quad-M, which offers a range of deployers that can accommodate one, two, or three PocketQube

satellites, respectively. These deployers have been designed to meet the same strict standards as other spaceflight hardware and undergo extensive testing to ensure their reliable and safe operation.

Innovative Solutions in Space (ISIS) is another manufacturer of PocketQube deployers, which offers deployer models such as the QuadPack and the QuadPackPlus. These deployers can accommodate up to four PocketQube satellites each and can be highly customized to meet specific mission needs. They are also modular, which allows users to swap out components with ease.

Other manufacturers of PocketQube deployers include NanoAvionics, which offers deployers for various satellite sizes, and Space Inventor, which offers deployers for both PocketQube and CubeSat satellites. Given the rising popularity of PocketQube satellites in recent years, it is expected that more manufacturers will enter the market in the near future, offering new and innovative deployer designs to cater to the evolving needs of the industry.

2. DESIGN AND PHYSICAL FRAMEWORK

2.1 Mechanical specifications

In order to ensure a successful launch of a satellite, it is inportant that all requirements set by the launch provider are met. This includes undergoing a series of tests for the alternative structure to be used, such as random vibration test, thermal vacuum bakeout, and shock testing. These tests are essential to ensure that the satellite's mechanical structure is capable of withstanding the harsh conditions of spaceflight. During the random vibration test, the satellite is subjected to a wide range of vibrations to simulate the launch environment. The purpose of this test is to ensure that the satellite's mechanical structure is capable of withstanding the intense vibrations that occur during launch. The thermal vacuum bakeout test, on the other hand, is designed to observe the behavior of the satellite's components and any potential outgassing in the vacuum of space. This test is critical in ensuring that the satellite can operate effectively in the harsh environment of space. In addition to these tests, shock testing is also a requirement set by the launch provider. This test simulates the shock and impact that the satellite will experience during launch and separation from the launch vehicle.

It is essential to ensure that the satellite's mechanical structure can withstand the shock and vibrations that occur during launh and separation. It is also important to note that the launch provider's standards and requirements must be strictly adhered to in order to ensure a successful launch. The alternative structure must pass all necessary tests and meet the launch provider's standards before it can be considered for use in the mission. Failure to do so could result in a failed launch and the potential loss of valuable resources, which can be detrimental to the mission's success.

Therefore, it is importatnt for the alternative structure to be thoroughly tested and assessed for its capability to meet the launch provider's requirements. This will ensure that the satellite is equipped with a reliable and durable mechanical structure, capable of withstanding the harsh conditions of spaceflight. In conclusion, meeting the launch provider's standards, to ensure the success of the mission and the protection of valuable resources. [8]

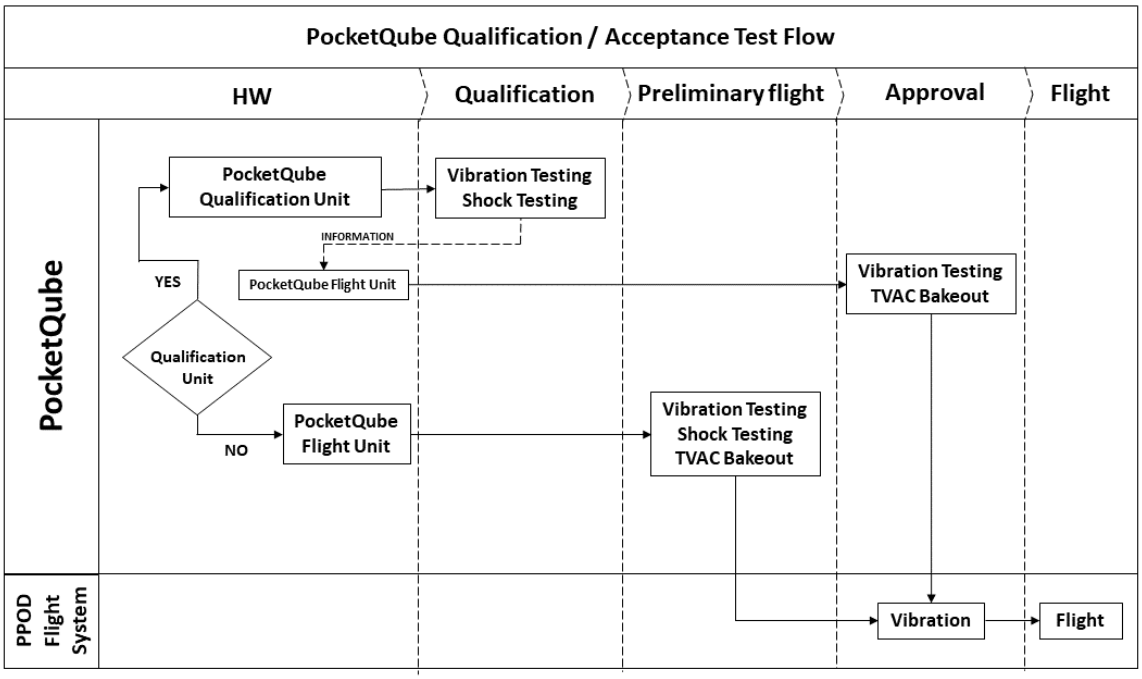

Figure 4: The PocketQube Design Specification, adapted from the CubeSat Design Specification REV 14.1 CP-CDS-R14.1

The mechanical structure of a satellite is a important component that plays a vital role in its functionality and overall success. Typically, these structures are pre-manufactured by certified companies such as AlbaOrbital, and they must be compatible with the deployer to ensure proper deployment in space.

2.2 Materials for the manufacture of structural frame

2.2.1 Aluminium alloys

PocketQube frames are a popular choice for satellite construction because of the various advantages that aluminum alloys offer. These include high strength-to-weight ratio, corrosion resistance, and ease of manufacturing. When it comes to selecting the right alloy for a PocketQube frame, designers must take several factors into consideration, such as the satellite's size and weight, the launch environment, and the desired level of durability and stiffness.

One of the most commonly used aluminum alloys for PocketQube frames is Al 6061, which is known for its excellent weldability and high strength. Additionally, this alloy is lightweight and has excellent corrosion resistance, making it ideal for use in space applications. Another popular option is Al 7075, which has even higher strength than Al 6061, but it can be more difficult to weld. Aside from the base alloy, designers can also add other elements to enhance specific material properties. Silicon can be added to improve casting properties, while magnesium can enhance strength and corrosion resistance. By adjusting the aluminum alloy's composition, designers can achieve the

desired properties for their PocketQube frames. In conclusion, selecting the appropriate aluminum alloy for a PocketQube frame is a imoportant decision that requires careful consideration of several factors. By choosing the right material, designers can ensure that the satellite will be able to withstand the challenges of launch and operate successfully in space.

Choosing a specific material for PocketQube must be approved by DAR - Deviation Waiver Approval Request, which is a formal document used to request a deviation from a requirement or standard. It is typically used when an organization cannot meet a specific requirement and needs to request an exemption from that requirement. It should include a detailed explanation of the deviation and the reasons why the organization cannot meet the requirement. The request should also include a plan for how the organization will mitigate any risks associated with the deviation. [8]

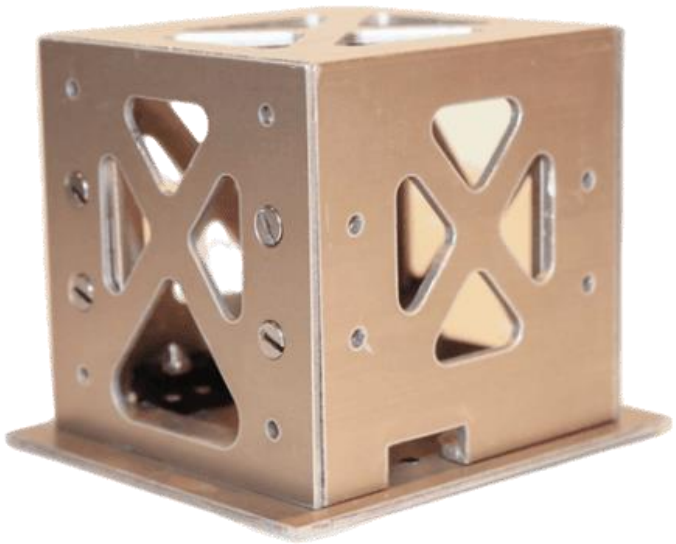

Figure 5: Aluminum frame of PocketQube by AlbaOrbital [31]

2.2.2 Metal 3D printing

3D metal printing has the advantage of providing almost the same properties as aluminum alloys, making it a viable option for PocketQube frames. This technology also offers greater design flexibility, allowing for the creation of complex shapes and geometries that may be challenging to achieve with traditional manufacturing methods. However, there are some drawbacks to using 3D metal printing for PocketQube frames. The process can be financially expensive due to the specialized equipment and materials

required. Additionally, the technology is not yet widely available and may not be accessible to all designers. As a result, designers must carefuly consider the cost and availability of 3D metal printing before deciding to use it as an alternative to aluminum alloys for PocketQube frames.

2.2.3 3D printing of plastic

The use of alternative materials for 3D printing of PocketQube structures requires careful consideration of challenges associated with transport and handling, launch environment, and on-orbit behavior. However, using these materials provides several advantages, such as adapting the complexity of the space structure, which is crucial in tailoring the satellite payload to suit its requirements.

Currently, the most popular materials for 3D printing are PLA or PETG, which are processed at around 250°C and used in open desktop printers. However, new materials are being developed to better handle higher temperatures. Exposure to UV radiation can cause damage to PLA materials over time and alter their characteristic behavior. This is an important consideration for 3D printing in space, as the harsh space environment can expose materials to high levels of UV radiation. The effects of UV radiation on PLA can lead to brittleness and decreased strength, which could compromise the integrity of printed structures. Therefore, when using PLA for 3D printing in space, it is important to consider the material's susceptibility to UV radiation and take measures to protect it from prolonged exposure.

Hence, it is necessary to choose the right printing material that can withstand these conditions. Apart from spaceflight, high-temperature plastics are extremely useful in other industries such as automotive and aerospace. However, printing these materials is not suitable for open desktop printers. To produce these high-temperature plastics, the heat must be concentrated and controlled. Fortunately, there are many manufacturers of printers suitable for this purpose, such as Roboze, INTAMSYS, Minifactory, or Stratasys. The most common types of high-temperature plastics produced by thermal extrusion include polyetheretherketone (PEEK), polyamide (PA), and acrylonitrile butadiene styrene (ABS). These plastics typically require processing at temperatures around 400°C, but the biggest challenge in manufacturing them is thermal management and achieving ideal material behavior.For educational purposes and laboratory PocketQube satellite production, only standard methods and materials, such as PLA, are suitable. [9] [10]

This is because these materials are readily available and easy to handle, making them ideal for learning and experimenting with 3D printing. Nevertheless, as technology advances, there is an increasing need to explore the use of alternative materials to optimize the performance of PocketQube satellites in space.

Figure 6: 3D printed educational model - AlbaOrbital (ABS) [31]

3. ELECTRONICS

3.1 OBC

The On Board Computer (OBC) subsystem is a critical component of a satellite, responsible for ensuring that all primary functions are performed correctly and implementing critical decisions while monitoring all subsystems on the satellite. It is composed of three main parts: a microcontroller, data storage memory, and I/O interfaces for communication. The OBC is responsible for processing data from the payload monitoring systems, collecting data from communication, and managing data storage. The processor used in OBC is linked with various sensors and actuators present on the satellite, enabling it to gather information for performing tasks and subsequently evaluating actions. Planning activities based on the number of tasks that need to be carried out is also an important part of OBC. The processor needs to be capable of executing programs reasonably well, with a relatively simple processor or microcontroller capable of handling basic satellite tasks such as power management, comunication, position control, etc. However, it is essential to have an adequate number of communication ports and protocols as the processor will need to communicate with various sensors and other processors. Satellites today use various types of microcontrollers including Raspberry Pi or Arduino, but standardized technologies utilizing "bare-metal C code" from the AVR, ARM, or Linux systems are preferred. NuttX is one company that has implemented Linux RTOS for PocketQube. [12]

The structure of OBC can be centralized or decentralized, with each having its own advantages and disadvantages. A centralized system is a traditional solution that is simpler and used more in small satellites. In this arrangement, the entire functionality of the satellite is centralized around one OBC, and all communication interfaces between subsystems pass through the OBC. If the OBC fails, the entire satellite mission is terminated, and the satellite stops functioning. The OBC acts as the master, and other slave nodes have a simple function. A decentralized system, on the other hand, is a more complicated solution where each subsystem is responsible for its internal functioning. Each system communicates independently with the communication system, having independent connections to the payload, power system, ADSC, and communicating with them in real-time. The decentralized system provides a more reliable solution to system failures, allowing for the continued operation of subsystems even if the OBC fails. However, it requires a higher level of complexity and coordination among the subsystems. In addition to the aforementioned advantages and disadvantages of the two OBC structures, there are other factors to consider when choosing a structure. For instance, a decentralized structure is more expensive than a centralized structure, but it provides greater reliability in case of system failure. A decentralized system is also more difficult to manage and coordinate, which could pose a challenge during the satellite's lifetime. When designing OBC, it is essential to consider the requirements of the mission

and the constraints that must be met. One constraint is the size of the satellite, which limits the amount of space available for OBC. Another constraint is the budget, which determines the resources available for designing and building OBC. It is essential to invest in high-quality OBC technology that meets the mission's requirements and constraints. [2] [13]

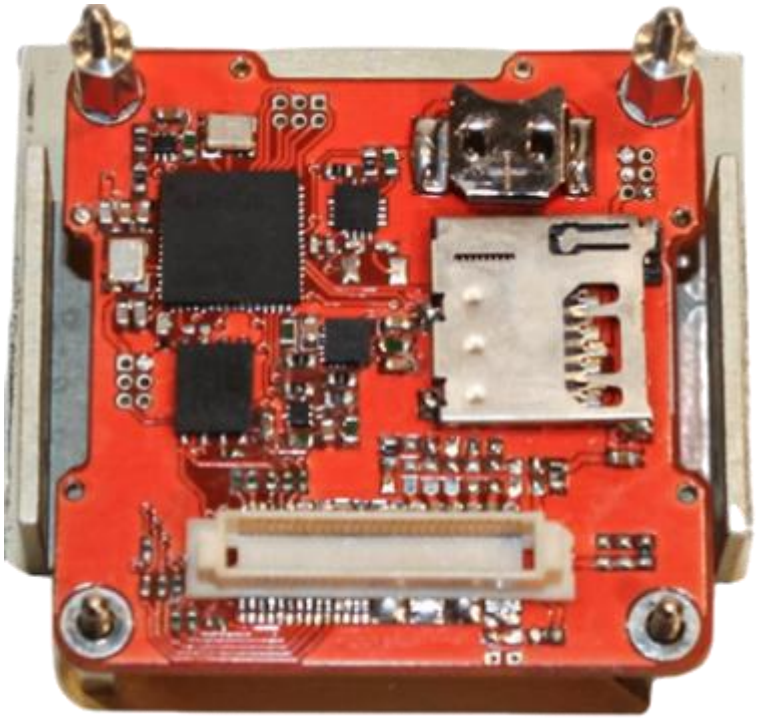

Figure 7: On Board Computer - Alba Orbital - TI MSP430 Microcontroller [30]

3.2 COM

Communication subsystems are the most critical parts of a satellite because they provide the only access to it. During a satellite's lifetime, communication links are used for commanding, telemetry acquisition, pointing, and firmware updating.

All radio frequencies used fall under the jurisdiction of the International Telecommunication Union (ITU), which divides the frequency spectrum into multiple categories. The bands most commonly used for satellite communication with a ground station are VHF (2m, 144MHz) and UHF (70cm,432MHz), L-band, and S-band. Amateur satellites usually try to get into amateur radio bands, where the allocation is easier than in commercial bands.

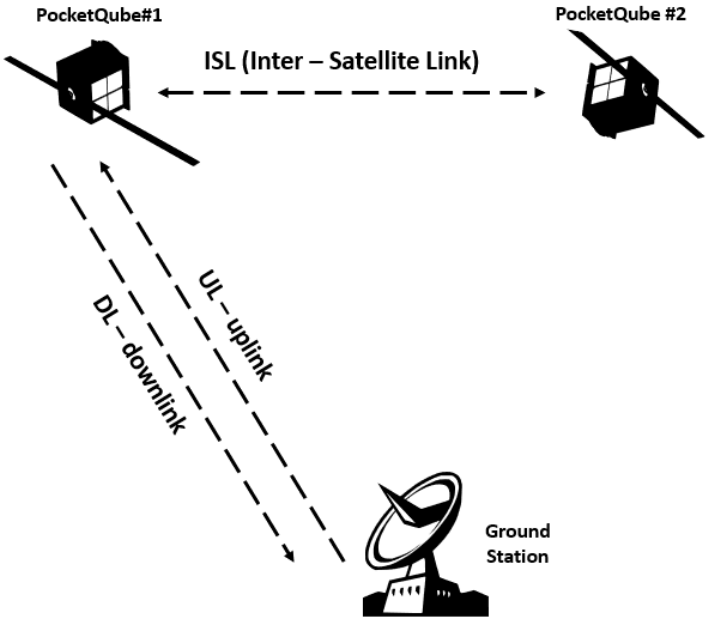

Figure 8: Communication scheme

When it comes to communicating with nanosatellites, a variety of protocols and modulation techniques are used to ensure reliable and efficient data transfer. At the physical layer (L1), two common modulation techniques are used: audio frequency-shift keying (AFSK) at 1200 baud and frquency-shift keying (FSK) at 9600 baud. AFSK involves shifting the frequency of an audio tone to represent digital data, while FSK involves shifting the frequency of the carrier signal itself. At the link layer (L2), the AX.25 protocol is often used. This protocol is widely used in amateur radio applications and provides a robust and efficient method for packet data transfer.

LoRa modulation is mainly used in PocketQube satellites where insufficient power is available (for PocketQube, power of hundreds of milliwatts is expected). LoRa has the advantage that we can also demodulate the signal below the noise floor (the signal-to-noise ratio can be negative). It is very slow in terms of transmission speeds - increasing the transmission time. There are several commercial manufacturers that currently offer LoRa modules - Aurel, Hope microelectronics, Insight SIP, etc.

In recent years, LoRa has become an interesting alternative for satellite communications. For example, a test was conducted where the maximum distance of the communication function using a stratospheric balloon was tested, which reached 832 km [15]. Recently, Lacuna Space's CubeSat satellite with LoRa communication technology has been launched [16], as well as another PocketQube with a LoRa transmitter, from the Spanish manufacturer Fossa Systems, which can communicate with their ground module. [17] [18]

3.3 **EPS**

The satellite's power system performs a major role in the mission, namely power generation, distribution, storage and control. These functions are necessary for all electrical requirements of the entire satellite, its subsystems as well as the payload. The main blocks are the solar panels that convert solar energy into electrical energy. Battery charge controllers, which are used to charge the batteries from the solar panels. Another element is the voltage regulators and the batteries themselves, which store the electricity. [14]

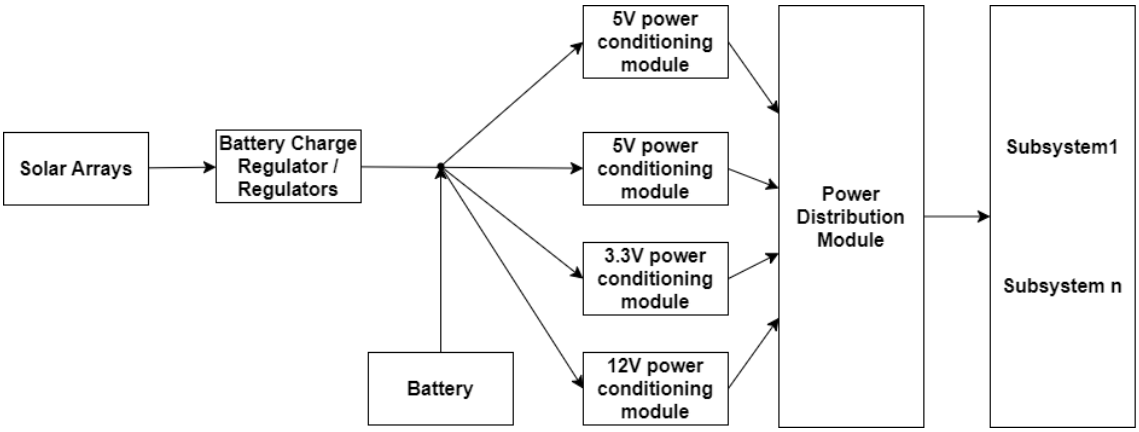

Figure 9: Nanosatellite power system architecture

Photovoltaic solar cells are the most widely used energy source in nanosatellites. Of the available technologies, (GaInP/GaAs/Ge) "triple junction" is used in miniaturized satellites. The theoretical efficiency of these panels is 33%, while in practice the efficiency reaches 28% to 30%.

But as for conventional polycrystalline silicon solar panels, which are much cheaper, these panels achieve efficiencies of 10% to 15%. This technology is particularly suitable for educational and demonstration purposes.

The limitations of solar cells are: non-energy generation during the eclipse cycle, degradation and inability to be used in deep-space missions. [2]

Since solar energy is not available during the entire satellite operation, the energy needs to be stored in batteries to guarantee the continuous operation of the satellite. The choice of battery and battery size should take into account several factors namely number of charge cycles, discharge, temperature ranges and power delivery requirements. Nickel-cadmium (NiCd), nickel-hydrogen (NiH2), lithium-ion (Li-ion) and lithium polymer (LiPo) batteries are used. Li-ion is the most widely used technology on nanosatellites, due to its high energy density and high voltage per cell. However, Li-ion batteries degrade in capacity with the number of charges/discharges and the amount of energy associated with a single charge. It is also important to monitor the temperature and the value of the

discharge current. Typical nominal cell voltage is 3.7-3.8V. They require additional cell balancing, precision charge control, MPPT for maximum solar panel efficiency, etc. Many nanosatellites, therefore, use older NiCd and NiMH batteries. These batteries are very resistant to cell overcharging, long term discharge, etc. The only drawback of this old technology is their low efficiency, weight and size. In this case, there will be used pack of NiMh batteries in proposed PocketQube.

There are two possible approaches to charging the batteries - DET - direct energy transfer and MPPT - maximum power point tracking. In DET, the connection between the solar panel and the battery is made using power semiconductors. The DET method uses sequential control. When using DET, the energy supply to the battery may be lower than that required for optimum function. A better battery management method is MPPT, which uses the operation of solar panels in the MPP section where the power delivered to the panel terminals is maximized. This method corresponds to the P_{max} value shown in the I-V characteristic.

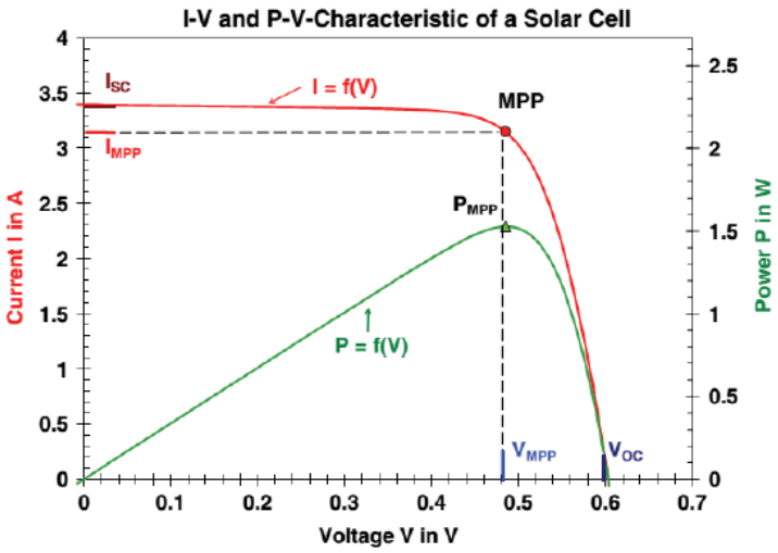

Figure 10: I-V characteristic of a solar panel [19]

The battery charge controller is usually implemented using a DC/DC converter in the control loop where the current or voltage is regulated. The controller works with the solar panel input at the MPP - using techniques (P&O, OC or IC).

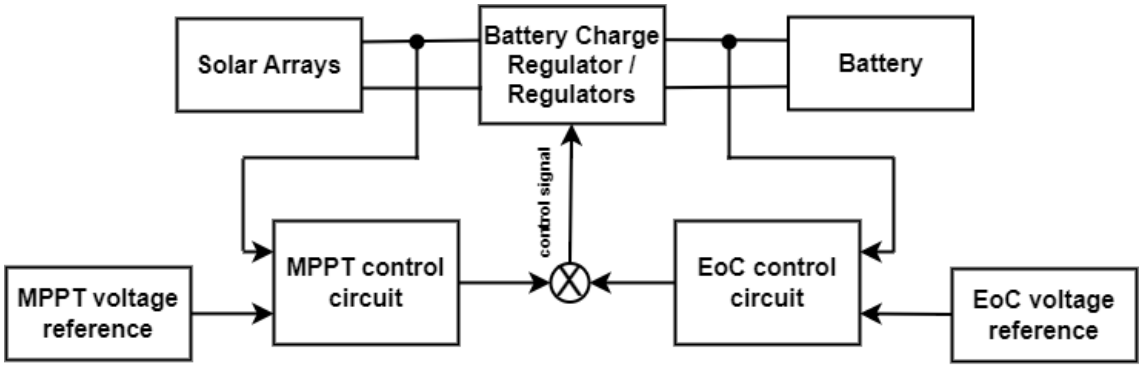

Figure 11: Diagram of nanosatellite control and control circuits

The EPS includes the ability to distribute power through several bus branches, for example 3.3V, 5V or directly to the battery voltage through protection circuits. These stable voltages are treated with DC-DC converters (switched or linear), short circuit protection (overvoltage) and temperature protection.

Another part of the EPS is the monitoring, the possibility of disconnecting the individual branches of the power supply input and output circuits and the watchog, which is used to reset the satellite, if necessary, in case of a fault or run-out of sleep, to the default state.

3.4 **ADCS**

Attitude determination and control system - used to stabilize, determine and adjust the position of the satellite as required. ADCS adjustment is needed to get the correct pointing for the payload, the correct rotation for the solar panels, but also for the satellite's antenna. The ADCS system of the satellite uses sensors (sun tracker, star tracker, horizon tracker, magnetometer, gyroscope) to decide the rotation and actuators to control the correct rotation direction. The ADCS setup targets accuracy, stability, rotation speed.

Active or passive attitude control can be used in nanosatellites. In the case of passive attitude control, it is by mounting permanent magnets on the structure, which generate a torque that tries to align in the direction with their local magnetic field. Active position control can be achieved by tri-axial stabilization (momentum wheels) that have the ability to perform maneuvers. These triaxial reaction wheels are at right angles in all axes. These reaction wheels need to be desaturated by a torque rod which gradually stops the reaction wheels without rotating the satellite.

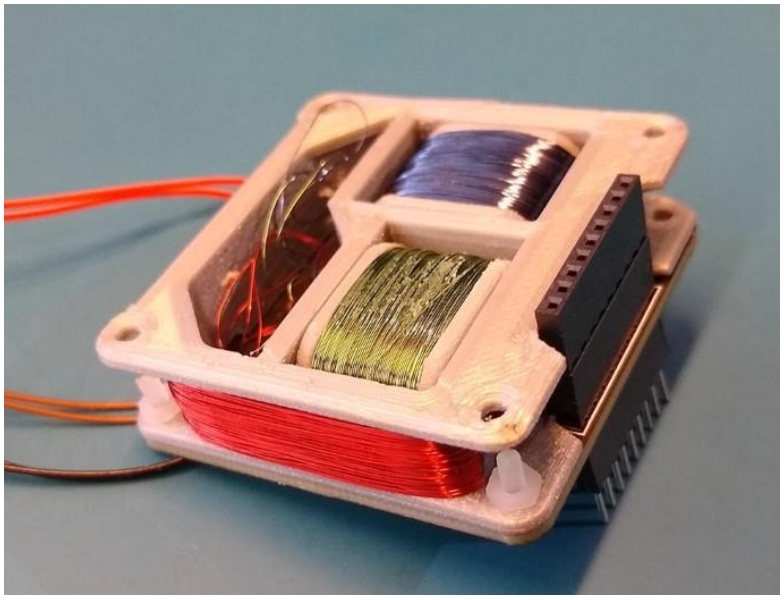

Figure 12: Mangetorquer for Delfi-PQ PocketQube satellite [7]

ADCS for nanosatellites (CubeSats) are commercially available, but they are not highly optimized for the PocketQube format. Precisely because of the small footprint of the PocketQube, even ADCSs must be of minimalist dimensions while maintaining sufficient strength for reliable attitude control. In this case, the biggest constraint comes from the power budget of the PocketQube. The ADCS can easily be the consumer of all the energy stored in the solar panels. Therefore, ADCS is only implemented on the satellite when it is needed.

Alba Orbital has developed the smallest ADCS on board the Unicorn-2 platform. They were the first to integrate an ADCS on the PocketQube, which contains torque rods (magnetorquers), reaction wheels, a sun sensor and a gyroscope to ensure reliable detumbling and precise pointing.

4. POCKETQUBE PROPOSAL

4.1 Mechanical construction

The educational PocketQube satellite will have a mechanical design made by 3D printing due to its good availability and low cost. The structure consists of a 2p skeleton (114x50x50cm) on which the solar panels will be mounted. Inside the skeleton of the satellite, OBC+COM circuit boards and a power module with batteries will be inserted. The individual modules will be connected by a common bus, via a 2.54mm pin rail, which can be layered on top of each other. This bus will be used for power distribution, communication via RS485 interface between the subsystems, which can be added in future, and IO pins of STM32.

The 3D model has been completed with M2 inserts for easy completion of the structure. After several iterations of the model, the final model was developed, where the bottom frame and top frame will serve as the basic skeleton to mount the side plates with solar panels and the bottom rail structure for the deployer. The final version of the frame design can be seen in the following picture. The actual design and dimensions of the PocketQube 3D model are attached.

Figure 13: PocketQube prototype in 2p format (CAD Autodesk)

Solar panels will be mounted on all tops of the pocketQube shell. PCBs will be layered inside the frame using connecting pins on standard rail (2.54mm pin size). This bus is including power supply branches, communication for individual subsystems and also unconnected pins or IO pins. This topology guarantees possible expansion and modularity of the whole system. The size of the individual PCBs is very minimized and limited by the internal dimensions. On the bottom board are placed rechargeable NiMh 2/3AAA battery pack. Dimension of PCBs is 42x42mm in PQ60 format for easy stack-on.

.

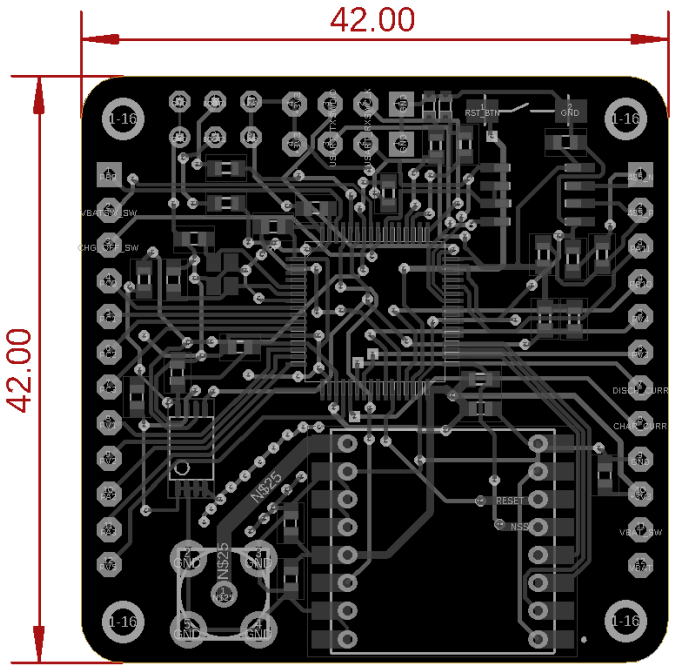

Figure 14: PCB dimensions for PocketQube – PQ60

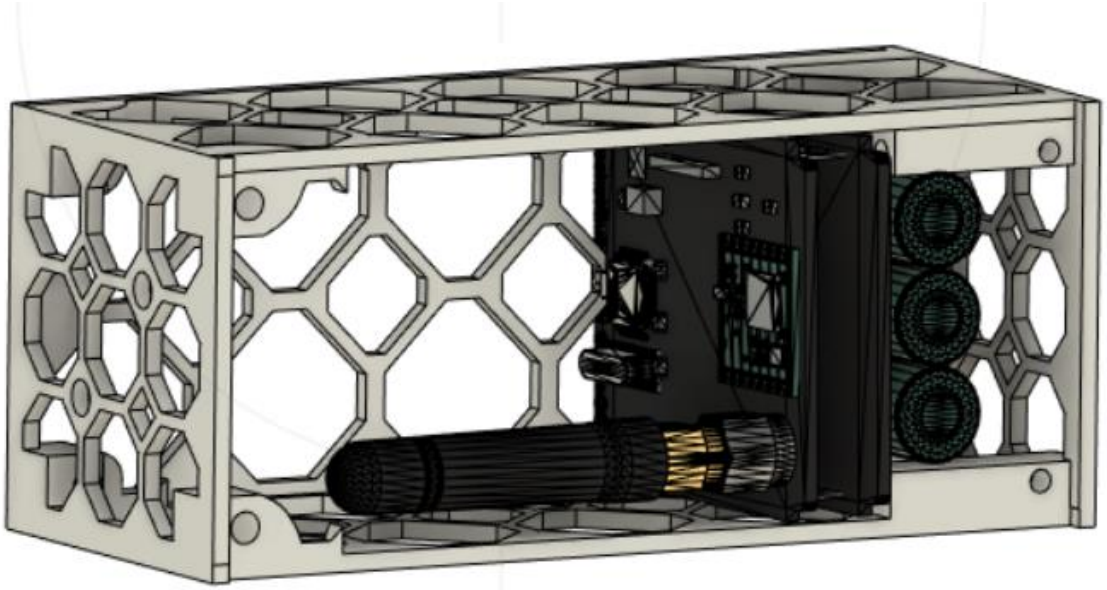

Figure 15: Model of the PocketQube 2p demonstrator with layered PCBs inside

4.2 OBC + COM

4.2.1 Communication module

When choosing a communication module for a small satellite for example as 1U CubeSat, there are plenty of communication schemes to choose from. They can use UHF transceivers, that are commonly used in Cubesats for communication purposes. They operate in the UHF frequency range, typically around 400-450 MHz, and are well-suited for Cubesat missions due to their compatibility with amateur radio frequency bands. They are providing reliable communication links, allowing for data transmission and reception between the Cubesat and ground stations or other satellites. This enables various mission operations, including telemetry, command, and payload data downlink.

These modules support modulation schemes such as FSK (Frequency Shift Keying) and BPSK (Binary Phase Shift Keying), which allow for efficient and robust data transmission. The modules are designed to operate efficiently and optimize power usage while maintaining reliable communication. Factors that must be taken in idea aresuch as size, weight, power requirements, and compatibility with the mission's communication protocol need to be considered.

Another choice in small satellites are S-Band transceivers, operating in the 2-4 GHz frequency range, offer higher data rates compared to UHF transceivers and find application in scientific missions, Earth observation, and high-resolution imaging. Notable example if Pumpkin CubeSat S-Band Transceiver. [42] [1]

In contrast, X-Band transceivers function within the 8-12 GHz frequency range and cater to advanced Cubesat missions with greater data rate and higher-frequency communication requirements. X-Band communication is commonly utilized for inter-satellite links, deep space missions, and high-resolution imaging. The GomSpace X-Band Transceiver stands as an illustrative choice for Cubesat X-Band modules. [43] [1]

In the case of communication modules for PocketQubes, which are smaller than Cubesats and have limited space for solar panels to harvest energy, there is a constrained power budget for the satellite system, namely the communication (COM) system. Consequently, the choice for the PocketQube satellite application leans towards utilizing LoRa modulation due to its low power requirements.

The manufactures, which are producing modules for LoRa modulation were mentioned in Chapter 3.2., which are offering variety of well available ICs.

Table 1: Comparison of most available LoRa RF modules[21][44][45][46]

Part name	max. link budget (dB)	RF output (dBm)	sensitivity (dBm)	RX current (mA)	Dynamic Range RSSI (dB)	size (mm)	frequency(Mhz)
RFM96W	168,0	20	-148	10,3	127	16x16	433
RF-LoRa-868	157	20	-130	10	127	23x20	868
RC-WLE5	x	18,5	-140	10	x	13x14,5	868
XTR-8LR-ENC	x	20	-126	16	x	35x18	868

Because of very good parameters of RFM96W/RFM98W which are the same, was this module chosen for this PocketQube proposal. It has very good max. link budget of 168dB and sensitivity of -148 dBm. Also it is most smallest module currently available.

The next-generation ICs, SX126x/SX127x, wich is also RFM9xW using, offer a significant reduction in power consumption, cutting it by approximately 50% when compared to a similar configuration featuring the SX1127x. To achieve greater transmission ranges, the focus is primarily on increasing the RF output power before considering an increase in the spreading factor. This approach aims to optimize the efficiency and effectiveness of communication while maintaining an optimal balance between power consumption and transmission range.

The RFM9x series operates on a LoRa (long range) basis in the unlicensed sub-GHZ ISM 433MHz and 868MHz bands. Interference immunity and long transmission are ensured by the Chirp spread spectrum method. Based on spread spectrum, two-way modulation communication works by spreading the narrowband signal on channels with more bandwidth. The transmitted signal has a low noise level, which ensures that it has a higher immunity to interference. LoRa provides many settings for the transmission parameters, namely: spread factor SF7-SF12. A higher spread factor means a higher range

but a lower transmission rate. The maximum size per message is 64. The aim of this kind of communication is to minimize the power consumption on the transmitter side when there are requirements to transmit data only at certain time intervals several times a day. LoRa transmission can be secured by encryption.

A distinction is made between LoRaWAN, which is a communication protocol, and LoRa, the physical layer within the LoRaWAN (MAC Layer). This thesis deals only with LoRa communication (Physical Layer).

The module operates at a frequency of 433MHz, with selectable spreading factor (6-12), bandwidth (31.25 - 125kHz), bitrate (73.24 - 9375 kpbs) and sensitivity of -118 to -140dBm.

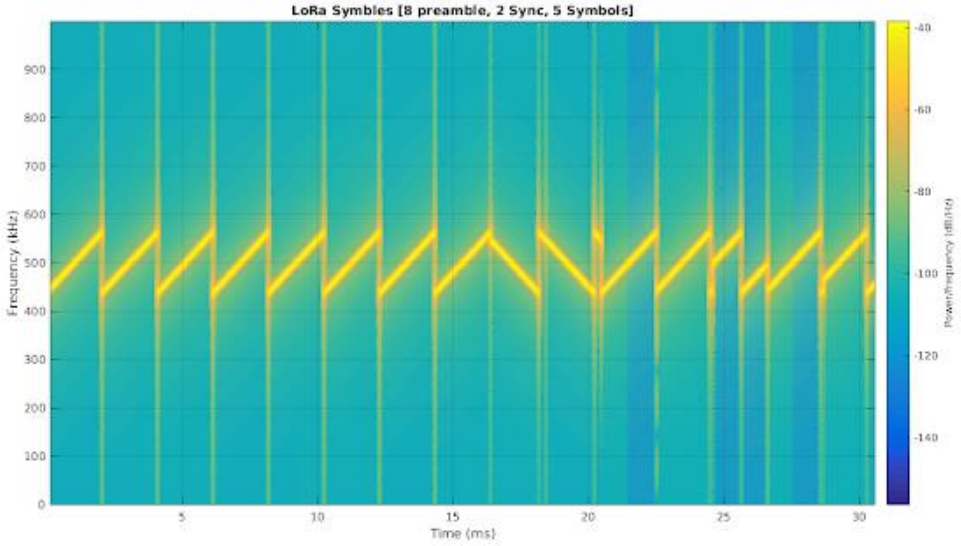

Figure 16: Lora symbols representation

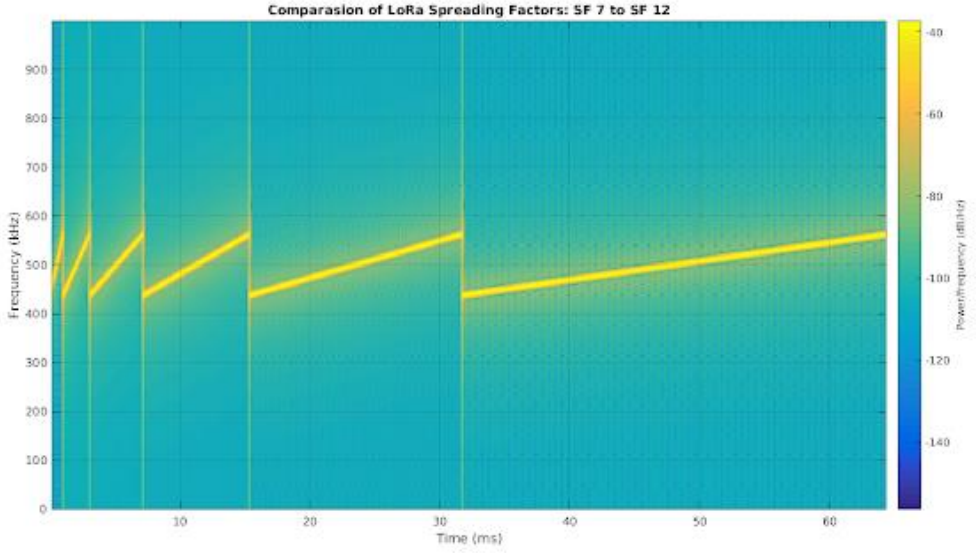

Figure 17: Representation of SF (Spreading Factors from SF7 to SF12)

The physical layer of LoRa consists of various elements, including 8 preamble symbols, 2 synchronistion symbols, physical payload, and optional CRC. The time taken by each spreading factor (SF) varies significantly. For instance, SF8 takes exactly twice the time of SF7, while SF9 takes exactly twice the time of SF8.There is a relation between the Symbol Rate (Rs), Bandwidth (BW), and Spreading Factor (SF). Specifically, Rs is equal to BW divided by 2 raised to the power of SF. This relationship means that higher SF results in higher over-the-air time, while lower SF yields higher data rates.

The RFM96W is a half-duplex, low-IF transceiver. The high-frequency signal is first amplified by the LNA. It is then split into a differential stage with down-conversion to I&Q components. The signal is then ADC converted and digitally demodulated. At this The signal level is converted through automatic frequency correction, RSSI (received signal strength indicator) and automatic gain control (AGC). The RF transmitter includes output amplifiers that can deliver up to +14dBm at the output. All parameters of the RF front-end and the digital state machine are configurable via the SPI interface. [21]

Figure 18: RFM98 communication module with pinout

4.2.1.1 Link Budget

When using a SX127x radio module for LoRa communication, we need to consider feasibility for using it for a LEO satellite application. SX127x typical power output for module can vary on the specific manufacturer and configuration. However, this module is commonly capable of transmitting up to 20dBm (100mW) of power. This is the maximum power specified by the module. It is importat to note that actual transmit power used in practical application can be adjusted based on the regulatory requirements, desired range and power consumption. This power can be configured in the software trought register settings of the module.

To calculate the link budget, we need to consider the following parameters: Transmit Power (PTx), which is the output power of the SX1278 transmitter module, Antenna Gain (GTx), with the gain of the transmitting antenna, Cable Loss (Lcable), considering the loss in the transmission cable/route connecting the transmitter to the antenna. Free Space Path Loss (FSPL), the loss of signal strength due to propagation over distance in free space, Antenna Gain (GRx): The gain of the receiving antenna,

System Noise Figure (NF): The overall noise figure of the receiving system, and Receiver Sensitivity (PSensitivity): The minimum power level at which the receiver can detect the signal. By considering these parameters, we can calculate the link budget and evaluate the performance of the communication system.

Lets estimate distance as the estimated line of sight horizon (2550km) of sattelite and its nominal orbit of 500km.

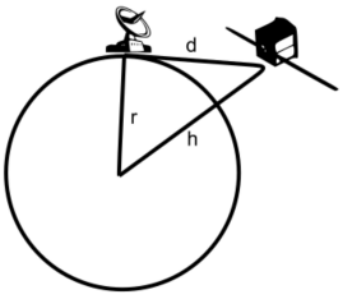

Figure 19: Estimation of calculating distances

It is calculated by this formula (pythagorean theorem), which is not considering terrain variations:

$$d^2 = (r + h)^2 - r^2 = 2 * r * h + h^2,$$

which can be simplified to:

$$d = 3{,}57 * \sqrt{h},$$

and now, it is possible to calculate FSPL (Free Space Path Loss), with formula:

$$FSPL\ (dB) = 20\log10(\mathrm{d}) + 20log10(f) + 20log10\left(\frac{4\pi}{\mathrm{c}}\right)(dB),$$

where: d is the distance between the antennas in meters, f is the frequency in Hertz and c is the speed of light in meters per second.

In this case, the distance between the antennas is given approximately to 2550km, which is equivalent to 2550000 meters, frequency is 433000000Hz:

$$FSPL\ (dB) = 20\log10(2550000) + 20log10(433000000) + 20log10\left(\frac{4\pi}{299792458}\right) = 145{,}39\ dB$$

Therefore the Free space path loss for a distance of 2550km at a frequency of 433 Mhz is approximately 145,39 dB.

For RX antenna Gain, we are considering a 2dBi, so therefore link budget calculation can be: 17dBm + 2 – 145,39 + 2 = -124,39 dBm.

When using a RFM96W, or basically SX127x module we can consider a receiver sensitivity around – 136dBm, leaving us with margin around 11,61 dB. Liink margin represents the additional power available to account for any additional losses or fades in the comunitacion link. The higher link margin, the better signal reliability. It means, that this form of communication model with SX127x module is theoretically accomplishable with a margin for external factors.

It is important to say, that a good choice of used antenna can increase margin and theroretically improve link budget for implementation LoRa communication in real application. [32]

It is also important to consider, that regional regulations and licensing requirements are essential for all amateur radio operations, to ensure legal an responsible use of the radio spectrum. In Europe, according to CEPT recommendation T/R 61-02, which is providing a guidelines for radio amateur operations, the maximum limit for power in ISM bands is typically 25 miliwatts (mW) or 14dBm. This power limit applies to the frequency range of 433,05 MHz to 434.79 MHz. [37]

4.2.2 MCU

When it comes to choosing low-power MCUs (Microcontroller Units) for IoT applications, several options are available that prioritize energy efficiency.

The Texas instruments The MSP430 stands out as a top choice for low-power embedded devices in IoT applications. With a maximum CPU speed of 25 MHz that can be adjusted for optimal power consumption, it offers a balance between performance and energy efficiency. The MSP430 incorporates six different low-power modes, enabling the disabling of unnecessary clocks and the CPU itself, effectively conserving power. Moreover, its swift wake-up times of under 1 microsecond facilitate prolonged sleep mode operation, resulting in reduced average current usage. With various configurations available, the MSP430 integrates a wide array of standard peripherals, making it a versatile and seamless choice for diverse IoT applications. [33]

Another choice in MCU selection for application in satellice with low power budget can be family of PIC32MCU, with its PIC32MX core, which incorporates a range of power management features that contribute to efficient power usage. These features include a low-power design, active power management, and power-down modes of operation. The core itself is designed as a static structure, allowing for the slowing down or halting of clocks (on the fly clock switching), when the system is idle, effectively reducing overall power consumption during periods of inactivity. These power-saving modes can be easily activated with a single instruction in software. [34]

Another choice in low power applications is Arduinos ATmega328P. By reducing the voltage supplied to the chip, the current draw can be significantly reduced. However, it's important to be cautious when lowering the voltage too much, as it may affect the microcontroller's behavior, particularly if the clock speed is not adjusted accordingly.

Reducing the clock speed is also the way. If timing is not critical and the project doesn't require high-speed processing, reducing the clock speed of the microcontroller can help decrease power consumption. The ATmega328P microcontroller has various built-in circuits that consume power. By selectively enabling and disabling these circuits through software control, it's possible to reduce power consumption. For example, disabling unused features like the analog-to-digital converter (ADC) can significantly cut down power draw. [35]

The STM32 family chip was selected as the microcontroller of choice due to previous experience with STM32CubeIDE and CubeMX development tools. Familiarity with these tools played a significant role in opting for this platform. Additionally, the availability of STM32 chips in the local Electronics store, along with their affordability, made them a convenient and cost-effective choice for the project.

For the main microcontroller STM32F103RBT6 is used, mainly due to the current availability of the F1 series in LQFP64 format, which will be mounted on a common board together with the communication module. The STM32F103xx offers a middle ground in performance with its parameters. The ARM®Cortex®-M3 32-bit CPU operates at 72 MHz with 64/128Kbyte flash memory, 20 Kbyte SRAM. Power supply voltage 2 - 3.6V. Sleep, standby and stop modes. 2x12 bit A/D converters and 9 communication interfaces (2xI2C, 2xSPI, 3XUSART). [22] The STM32F10xxx devices provide three low-power modes to optimize power consumption. The first mode is sleep mode, where the CPU clock is turned off while all peripherals, including important core peripherals like NVIC and SysTick, remain operational. The second mode is stop mode, in which all clocks are stopped, effectively pausing the device's operation. Lastly, the devices offer standby mode, where the 1.8V domain is powered off completely. These low-power modes allow for efficient power management and help extend battery life in applications utilizing the STM32 family of microcontrollers. This microcontroller, as well as the communication module, will be connected to a common bus.

4.2.3 EEPROM

Data measured from analog-to-digital converter can be stored in memory. The most available memory types with reasonable size was compared in table below and EEPROM with better parameters was chosen. The EEPROM 24AA512, manufactured by Microchip Technology, is a widely used EEPROM chip with a capacity of 512 kilobits or 64 kilobytes. It utilizes the I2C communication interface, allowing for easy integration with other devices on the same bus. The EEPROM is organized into multiple memory pages, typically 128 bytes each, enabling efficient data storage and retrieval. It supports both byte-level and page-level write operations, with excellent data retention for up to 200 years. With a high write endurance of at least 1 million write cycles, the 24AA512 offers reliable performance. It operates within a wide voltage range of 1.8V to 5.5V, making it compatible with various systems. EEPROM is in TSSOP8. [24]

Table 2: EEPROM comparison and parameters of choosen 24FC512 memory [24] [53]

Part name and Manufacturer	Memory array (Kbit)	Power supply (V)	Page writing time (ms)	Cycles	Read current (mA)	Write current (mA)	Standby (µA)
M24C32 (ST)	512	1,7-5,5	5	4 000 000	2,5	5	4
24FC512 (Microchip)	512	1,7-5,5	5	1 000 000	0,4	5	0,4

4.2.4 RS485

To facilitate the integration of future expanding subsystems, an internal bus protocol, RS485, has been chosen. The RS-485 standard will be utilized for internal communication between the systems, connecting them through a shared bus. This implementation ensures a reliable and efficient means of data exchange within the system, accommodating the potential addition of new subsystems in the future. The selection process for choosing the appropriate microcontroller was influenced by two key factors: local availability and suitability for low-power applications. Local availability played a role of choosing. Finally the MAX481 in SOIP8 package was chosen, which is a low-power transceiver designed for RS-485 and RS-422 communication. It features one driver and one receiver.

The MAX481 allows high-speed data transmission up to 2.5Mbps. It draws between 120µA (TX) and 500µA (RX) of supply current and has a low-current shutdown mode consuming only 0.1µA. The driver outputs have short-circuit protection and thermal shutdown circuitry. The receiver input has a fail-safe feature ensuring a logic-high output when the input is open circuit. The MAX481 is suitable for half-duplex applications and operates from a single 5V supply.

The integrated circuit (IC) is incorporated into the OBC+COM board and has dedicated pins on one of the two headers. These pins include 485_N, 485_P, and Enable, which are strategically placed for onvenient scalability in the future.

Table 3: Comparison of RS485 drivers [39] [40] [41]

Part no.	Transmit speed (Mbps)	Current TX (mA)	Current RX (mA)	ShutDown current (µA)
MAX481	2,5	0,12	0,5	0,1
ISL3179E	40,0	2,6	2,8	0,4

SP3483	0,25	1,5	2,0	10,0

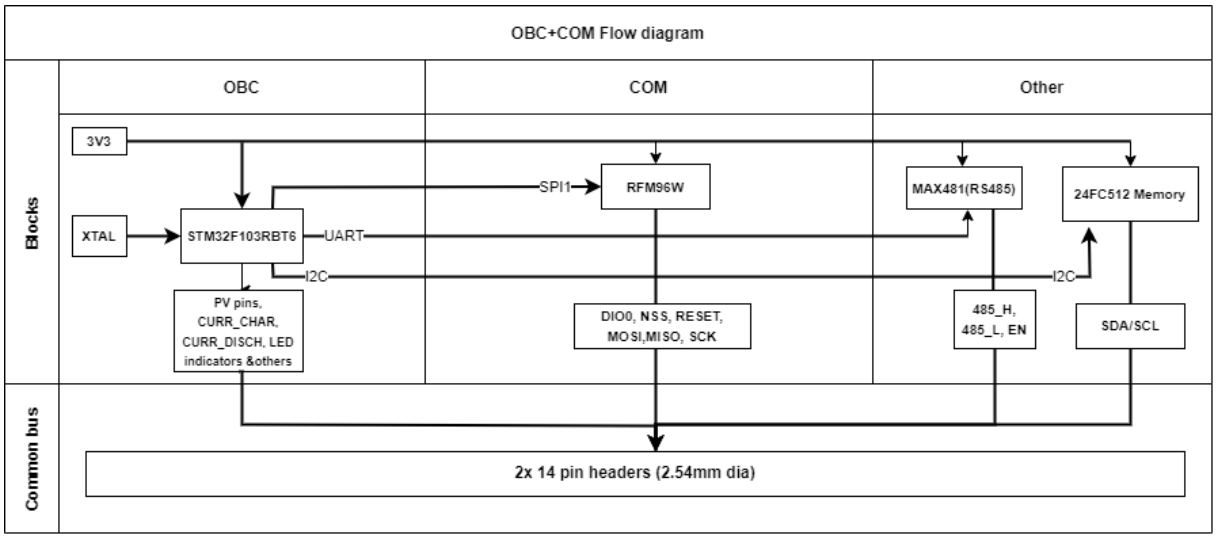

Figure 17: Simplified OBC+COM block concept

4.3 EPS

Proposal of EPS is shown in EPS circuit diagram in Figure 19 and complete schematics and PCBs can be found in Appendix

4.3.1 Photovoltaic panels and batteries

Since many of the locally available photovoltaic panels in a reasonable price range were not available, solar panels from the Chinese wholesaler Aliexpress were chosen 44x24 mm panels at 5V/30mA. [26] These are the declared parameters from the manufacturer in MPPT. When configuring 2x2 panels mounted in series, each panel generates 5V with a current of 30mA. When connected in series, the total voltage adds up, resulting in a configuration that produces 10V. Despite the increase in voltage, the current remains the same at 30mA.In the case of 3x4 panels mounted in series, each panel generates 5V with a current of 30mA. Connecting them in series results in a total voltage of 15V. Similar to the previous configuration, the current remains unchanged at 30mA. Real application can be presented on Figure 18. Real parameters are unknown, which is acceptable for demonstration purposes. In laboratory experiments, satellite will be alway powered by external power supply.Solar panels will be individually make a panels of two and four on each side of satellite as in Figure 18.

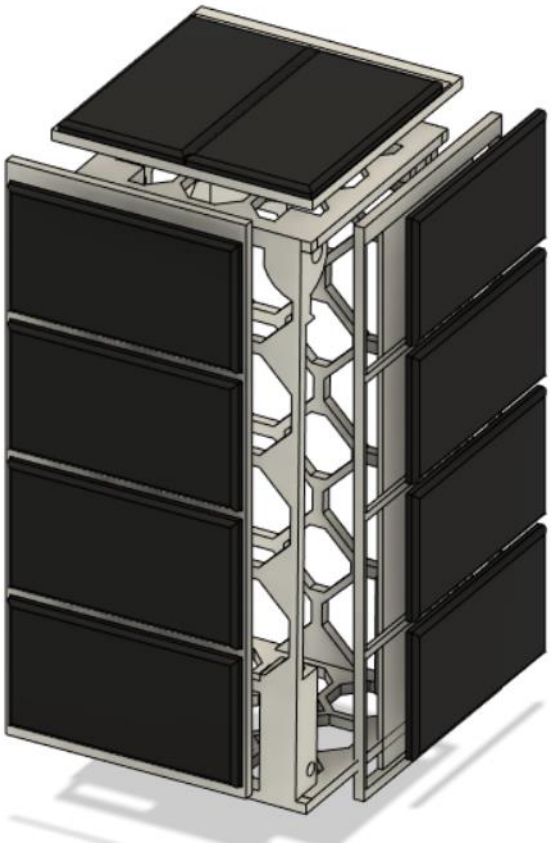

Figure 18: Solar panels mounted on chassis

The solution for PV panel connection and battery charging is to maintain the simplicity and small size of the PocketQube by using a direct connection through protection circuitry. A Schottky diode is frequently employed in solar panel setups to inhibit the flow of reverse current from the battery or load back to the solar panel during periods of non-production. It is connected in a configuration known as "reverse blocking“. This setup ensures that current flows from the solar panel to the battery, enabling charging. However, when the solar panel is not generating power or its output voltage falls below the voltage of the battery or load, the Schottky diode prevents any reverse current from flowing back from the battery to the solar panel. A battery pack connected, consisting of 3x 1,2V batteries with 600mA each, gives a total maximum voltage of pack 3.6V. Charging and discharding path is also protected with polymer fuses.

4.3.2 Sensing and regulating

The current sensing for the battery and solar panels is handled by the ACS712 circuit from Allegro. It was chosen based on a comparison with other current sensing ICs, which you can see below in this paragraph.The ACS712 incorporates a precise Hall sensor circuit with a copper conduction path near the die surface, enabling it to generate a proportional voltage in response to the applied current. The device's accuracy is enhanced by the close proximity of the magnetic signal to the Hall transducer. With a low-offset, chopper-stabilized BiCMOS Hall IC, the ACS712 delivers a precise and proportional output voltage. It offers a positive slope output when current increases

through the primary copper conduction path, which is dedicated to current sensing. The device features a low internal resistance of 1.2 mΩ, ensuring minimal power loss. Additionally, the copper conductor's thickness allows the ACS712 to withstand up to 5× overcurrent conditions. Electrical isolation is achieved by isolating the conductive path terminals from the sensor leads, eliminating the need for expensive isolation techniques. The ACS712 is packaged in a small surface mount SOIC8 package.

This is why the ACS712 was chosen for current sensing, in addition to the fact that the local supplier had it in stock. The following table presents its parameters alongside those of its competitors.

Table 4: Comparison of current sensing ICs [25] [47] [48] [49]

Part name and Manufacturer	Accuracy (%)	Current draw (mA)	Sensitivity (mV/A)	response (us)
ACS37010	1,5	18	26,4	1,3
MCS1806	2,5	10,5	264	5
CT452	1,0	9,0	667	0,3
ACS712	1,5	3	185	5

When it comes to voltage stabilization, there are two approaches available: linear and switched. Linear voltage regulators employ a linear pass element to continuously adjust the input voltage and provide a stable output voltage. They offer simplicity, low noise generation, and fast response. However, they suffer from power dissipation, lower efficiency, and a limited voltage range. On the other hand, switched voltage regulators use a switching element to rapidly switch the input voltage on and off and filter it for the desired output voltage. They excel in high efficiency, a wide input-output voltage range, and higher power handling capability. However, they are more complex, introduce more output noise, and have a slower response time. The choice between linear and switched voltage regulators depends on factors such as efficiency, power handling, voltage range, noise sensitivity, and the cost of the application. Also as EPS board is proposed to be 42x42mm small, it is more resasonable to use linear voltage stabilizer.

It will use a simple linear voltage regulator to stabilize the voltage in the EPS part. The power supply branches will be very simplified, divided into two namely a stabilized 3.3V branch and one unstabilized branch.

To power satellite from a 3.6V battery, 3.3V linear regulator is needed that can handle the combined maximum current draw of running devices. Adding up the maximum current values, total consumption is: 100mA (RFM98W) + STM32 50mA (active peripherals) + 5mA (EEPROM) + 10mA (RS485) = 165mA.

Therefore, a linear regulator capable of supplying at least 165mA of current is needed. It's recommended to choose a linear regulator with a slightly higher current rating to provide some margin and ensure stable operation.When selecting a specific linear regulator, consider factors such as dropout voltage, thermal dissipation, and any additional features required for your application. Popular options for low-power applications include regulators like the LM1117 or the MCP1703.

LM1117 800-mA, Low-Dropout Linear Regulator was choosen for this application as simplest solution. To ensure good thermal management and ensure efficiency, power dissipation P_d of the LM1117 linear regulator can be calculated as:

$$P_d = (V_{in} - V_{out}) * I_{load},$$

where V_{in} is the input voltage 4,8V, V_{out} is the output voltage 3,3V, I_{load} is load current, let assume 0,3 with a reserve.

$$P_d = (4{,}8 - 3{,}3) * 0{,}3 = 0{,}45W$$

If the LM1117 voltage regulator for 3V3 in the TO-252 package has a thermal resistance of 45.1 °C/W (as specified in the datasheet)[50], it means that for every watt (W) of power dissipated, the junction temperature of the device will increase by 45.1 degrees Celsius (°C) above the ambient temperature. To calculate the approximate junction temperature rise, is formula used:

$$\Delta T_j = \mathrm{P}_d * \mathrm{R}_{\theta \mathrm{JA}},$$

where ΔT_j is the junction temperature rise, P_d is the power dissipationθJA is the thermal resistance (45.1 °C/W in this case). Let's take the previous example where Pd is calculated as 0,46W:

$$\Delta T_j = 0{,}45 * 45{,}1 = 27{,}06°C$$

Therefore, the approximate junction temperature rise would be around 27,06 °C above the ambient temperature for the given power dissipation of 0,45W. This is an estimation, and the actual temperature rise will depend on various factors such as the ambient temperature, PCB layout, and heat sinking. If needed, a heatsink can be used in future.

Overal function of EPS is shown in Figure 19 describing basic concept iplementation.

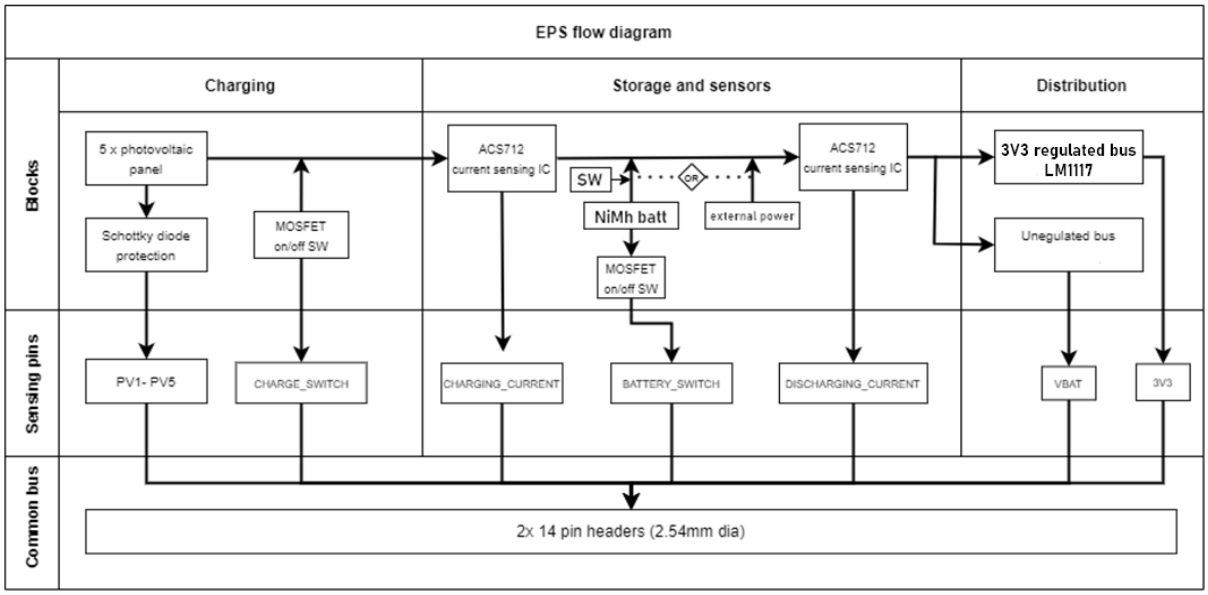

Figure 20: Block concept for EPS

4.3.3 Power Budget

4.3.3.1 Model situation

As there was mentioned earlier in Chapter 4.3.1 of EPC proposal, cheap solar panel from unknow supplier are used. This PocketQube proposal will be used in lab enviroment, but it is also required to calculate the power budget, especially if it is possible to charge batteries used in the proposal. To determine if the solar panel configuration can charge a 3.6V battery with a current rating of 600mA, we need to consider the voltage compatibility and the available charging current.

The total voltage output of the solar panel configuration depends on the series connection. As mentioned earlier, for the 2x2 configuration, the total voltage is 10V, and for the 3x4 configuration, the total voltage is 15V. To charge a 3.6V battery, you would need a charging voltage that is higher than the battery voltage to overcome any losses in the charging circuit. Typically, a charging voltage of around 4.2V is used for a 3.6V battery. Given the voltage output of the solar panels, it is necessary to use a voltage regulator or a charge controller to regulate the voltage and ensure it is suitable for charging the battery. The voltage regulator or charge controller can step down the higher voltage from the solar panels to the appropriate charging voltage for the battery.

Regarding the charging current, if each solar panel in configuration can generate current of 30mA, the total current for the 2x2 configuration would be 2 panels * 30mA = 60mA, and for the 3x4 configuration, it would be 3 panels * 30mA = 90mA. Since the battery has a current rating of 600mA, both configurations can provide sufficient current for charging the battery. In summary, the solar panel configurations you described (2x2 and 3x4) have the potential to charge a 3.6V battery with a 600mA current rating. However, it is important to use a voltage regulator or charge controller to adjust the voltage output from the panels and ensure the charging current is properly regulated for safe and efficient battery charging.

4.3.3.2 Real application in space

Let consider a PocketQube 2P satellite placed in a polar Low Earth Orbit (LEO) with a period of approximately 90 minutes. In this model scenario, let's assume that model situation with all active subsystems can be consumption around 1000mW, after simplicing, the total consumption of systems can be reduced to 125mW. Let consider a battery of capacity 4000mWh. When using a commercialy made solar panels, for example manufactured by AlbaOrbital, with prices starting from £4,999.00. The panel's characteristics are as follows: Operating under 1 sun, AM 1.5G conditions (1000 W per square meter), short-circuit current = 31mA, short-circuit voltage = 15.12 V, current at the maximum power point = 28 mA, voltage at the maximum power point = 13.14 V and maximum power = 368mW.

When considering 9 panels used, as satellite is rotating randomly, only 2,25 panels will be exposed to sunlight. Ttotal maximum power will be 368mW x 2.25 = 828mW. In

practice, we assume that the average power utilization is around two-thirds of its optimal capacity. So, the effective power would be 828mW * 0,66 = 546mW. Considering the satellite's orbit, it spends two-thirds of its time in the illuminated zone and the remaining one-third in the eclipse zone. As a result, the power of 546mW will be available during the lighting phase, while it will be 0mW during the eclipse phase. To calculate the average power over a complete orbit, we multiply the power in the lighting phase by its duration (0,66) and add it to the power in the eclipse phase (0mW) multiplied by its duration (0,3). Therefore, the average power throughout an orbit will be 546mW * 0.66 + 0mW *0,33 = 360mW. This was an example where fully charged battery is assumed.

During the first orbit, the solar panels supply an average power of 546mW during the lighting zone. As a result, we need to draw 454mW from the battery to account for the total power consumption of 1000mW when the repeater is active. The duration of the lighting zone in this orbit is approximately 1 hour, during which the satellite consumes 454mWh of energy. This leaves the battery with 1546mWh of remaining capacity, ensuring that it does not discharge more than 50%. [52]

It should be noted that this calculation assumes continuous activity of the repeater throughout the lighting zone. During the eclipse rely only on the battery. We need to utilize 1000mWh from the battery, while 1546mWh remain in the battery after the lighting zone. In the half-hour eclipse period, approximately 500mWh would be consumed, resulting in the battery having 1046mWh of available capacity, considering the 50% charge threshold.

During the second orbit, the satellite re-enters the light zone, and the solar panels once again provide an average power of 546mW. We need to draw 454mW from the batteries to meet the power requirement. Throughout the hour in the illuminated area, the satellite consumes 454mWh from the battery, leaving it with a remaining capacity of 1046mWh - 454mWh = 592mWh. Upon returning to the eclipse zone, the batteries once again supply the required 500mWh of power for the half-hour duration, resulting in a remaining capacity of 592mWh - 500mWh = 92mWh. For the third orbit, the satellite re-enters the illuminated area. With the available 92mWh of capacity to ensure it does not fall below 50% charge, this allows for approximately 12 minutes of operation, based on the power consumption rate of 454mW. Operating for a total of 3 hours and 12 minutes, comprising 1 hour in the first orbit, 30 minutes in the eclipse phase, 1 hour in the second orbit, 30 minutes in the eclipse phase, and 12 minutes in the light part of the third orbit.

When putting radio module to sleep mode, we can assume that During the hour that the satellite is in the light area, which occurs approximately once per orbit, the battery charges at the maximum rate allowed by the solar panels. Assuming a charge efficiency of 90%, the theoretical maximum limit for charging would be (546mW - 125mW) x 0.90 = 379mWh. Therefore, fully charging half of the discharged battery would require approximately (2000mWh / 379mWh) = 5.28 hours, equivalent to 5 hours and 17 minutes. This corresponds to approximately 5.2 orbits, with each orbit providing 1 hour of net charging time. Additionally, it would take an additional 7.8 hours of inactivity (5.2 orbits

x 1.5 hours) to return to the initial situation of full charge. In conclusion, this results in an activity time of 29% (3 hours and 12 minutes out of the total 11 hours). From the same geographical position, the satellite can be used four times a day, arranged in two groups of two consecutive passes. [52]

5. COMMUNICATION

5.1 Communication library

The SX1278 library is compatible with various LoRa modules, meaning it can be used with different hardware implementations based on the SX1278 chip. This versatility allows the library to work with a wide range of devices that incorporate the SX1278 transceiver. [27]

It is designed to communicate with the LoRa module using SPI (Serial Peripheral Interface) protocol. The code includes various functions that perform different operations such as reading from and writing to the module, configuring its settings, and transmitting and receiving data packets.In the first paragraph, the code defines several functions for reading and writing data to the SX1278 module via SPI. The functions SX1278_SPIRead and SX1278_SPIWrite handle single-byte read and write operations, while SX1278_SPIBurstRead and SX1278_SPIBurstWrite handle multiple-byte burst read and write operations. These functions utilize the hardware-specific SPI commands provided by the SX1278_hw module.

In function SX1278_config,, which is responsible for configuring the SX1278 module various parameters such as frequency, power, bandwidth, coding rate, and spread factor are set. It also initializes the module in LoRa mode, sets the synchronization word, and configures the modem and packet length. Additionally, it puts the module in standby mode, ready for further operations.

LoRa packet transmission and reception are handled by SX1278_LoRaEntryRx function prepares the module for receiving data packets by configuring the necessary settings and entering RX mode. It waits for the reception to start and updates the module's status accordingly. On the other hand, the SX1278_LoRaEntryTx function prepares the module for transmitting data packets. It sets up the required parameters and enters TX mode. The SX1278_LoRaRxPacket and SX1278_LoRaTxPacket functions handle the actual reception and transmission of data packets, respectively. They utilize the FIFO registers to read and write packet data. SX1278_available and SX1278_read functions provide a way to check for and retrieve received data from the module. Also it is possible to calculate RSSI with SX1278_RSSI. [27]

5.2 Communication testing

Whole project was written in programming language C. It was developed in STM32CubeIDE and pins were configured in STM32CubeIDE FW_F0 V1.11.3. To verify LoRa communication, at first stage of project, there was developed Ground station board (Appendix G-I), where simple transmission of communication was set. One development board worked as master and the other worked as slave. The master sends data to the slave device periodically in time. The boards had the same firmware

loaded..The mode in which the module is currently operating (Slave/Maseter) can be changed by a button connected to PC13 (mode input).

The RFM98W module communicates with the STM32 using the SPI protocol which uses pins PA5, PA6, PA7. Additional pins for communication logic are also connected - PB6, which is connected as DIO0 and PC0 as RESET. DIO0 is used to set the LoRa state of the module so that if its logic level is "high", data is received and the MCU can read it. In this project polling (manually detecting if DIO0 is in logic level "high") has been used. For uart serial communication the standard (115200 8N1 (115200 bps, 8 bit/frame, no parity and one stop bit) is chosen. As for antenna on dev board was chosen simple Linear polazired, with gain of 2dBi (zenith), impedance of 50Ω, with SMA connector, which can be a good solution for testing in laboratory environments. If needed, to SMA connector can be mounted additional antenna, for example dipole antenna, wchi can be mounted on external frame of structure.

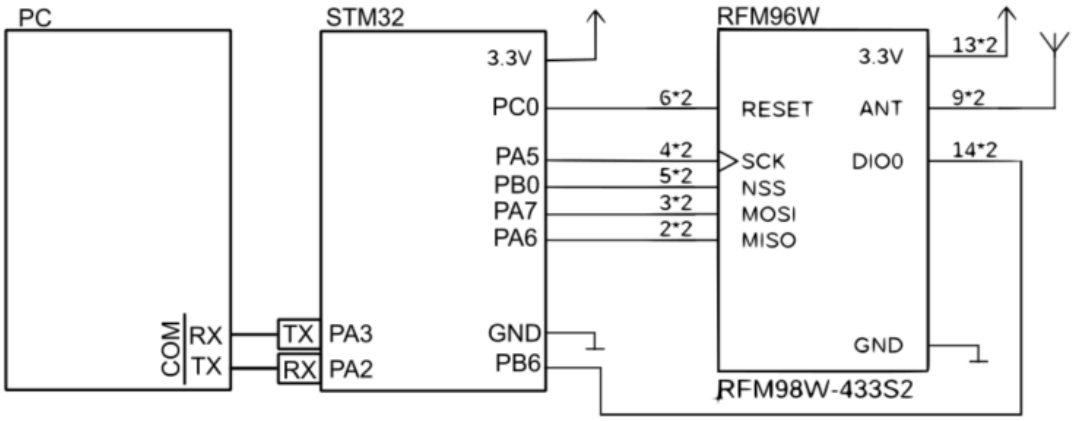

Figure 21: Simplified model of ground station flow with representation of connections

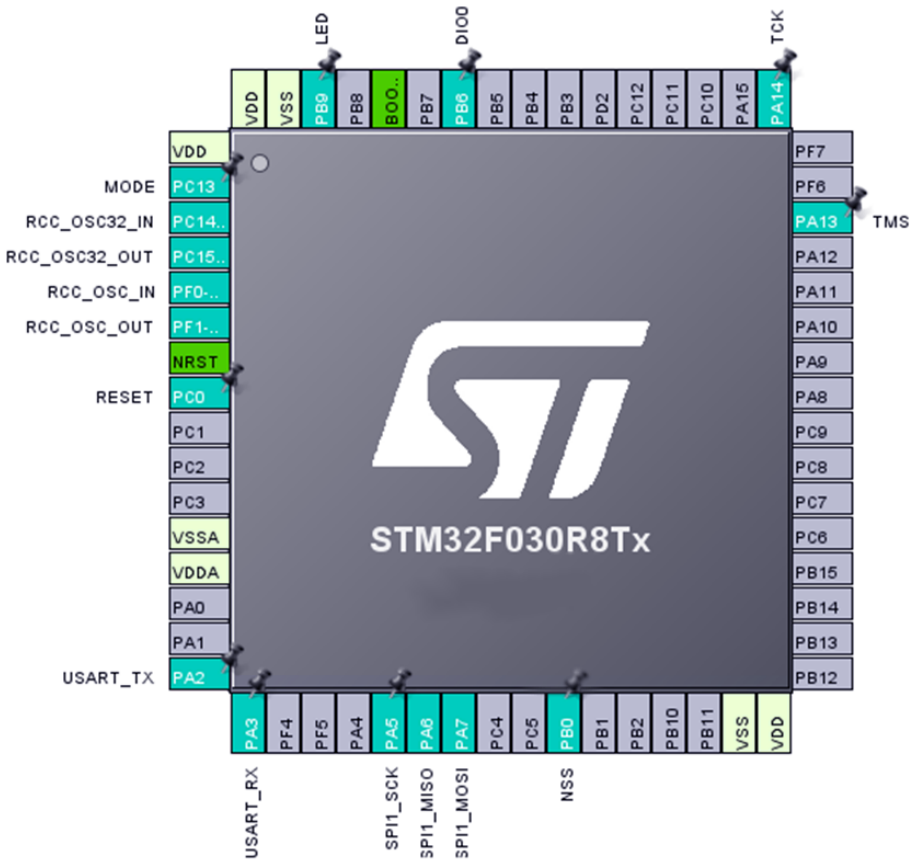

Figure 22: CubeMX representation of defined pins while testing between two Nucleo Boards

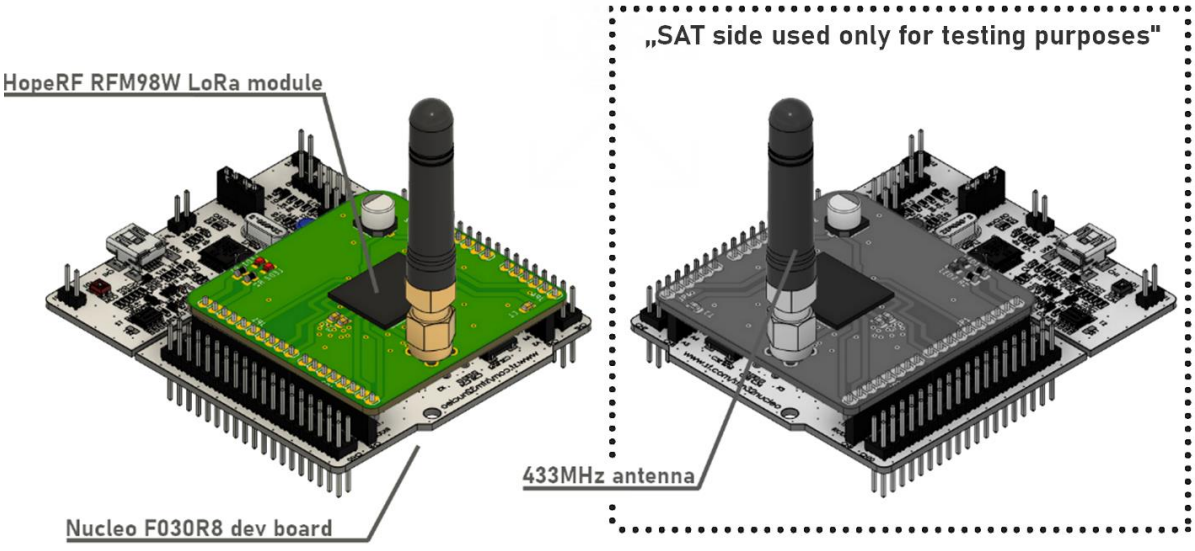

Figure 23: Communication demonstration modules between identical development boards (Nucleo), with prototype board usingLoRa module

6. GROUND STATION FW

6.1 Introduction

Whole system is working on upgrade project based on communication testing between two identical nucleo boards. Main core is running on internal clock with 8 MHz oscillator, which is then rised to 48 MHz with internal PLL. Commands are sent from PC or to PC via USART via internal ST-LINK programmer. Ground station is using DMA (Direct Memory Access)) on USART2s RX (receive) functionality. DMA is providing feature in MCU, which can allow direct data transfering between pperipherals and memory, without the involvement of the CPU.

In this case, is DMA1 Channel 5 tranfering data from USART2 pheripheral source to a specific memory location. This is called „peripheral to memory“ tranfer. When USART2 receives data, instead of the CPU being involved in each data transfer, the DMA controller takes over and transfers the received data directly from the USART2's data register to the specified memory location. This offloads the CPU from performing repetitive and time-consuming data transfer tasks, allowing it to focus on other operations. So it can achieve efficient and high-speed data transfers, especially in scenarios where continuous data reception is required, such as serial communication. It improves the overall performance and responsiveness of the microcontroller by reducing CPU load and increasing data throughput.

As it was said in Chapter 6.1, the Ground station is using several GPIO pins, providing acces to external device (LoRa module).

NVIC (Nested Vectored Interrup Controllers) are key components responsible for managing interrupts and handling interrupts from various peripherals. Some of main interrupts that are running on Ground station is Time base: Systém tick timer, The time base in STM32 microcontrollers is a mechanism used for generating regular time intervals. One commonly used time base is the system tick timer. Its a hardware timer that generates interrupts on fixed intervals, providing precise time reference for various operations. The system tick timer is driven by a high-frequency clock source and can be used for tasks like time delays, scheduling, and measuring time intervals. When an interrupt is triggered by the system tick timer, an associated routine is executed to perform specific actions. It helps manage time-related operations and synchronization within the microcontroller, enhancing overall functionality. Another, DMA interrupt, which is arranging interrupts to notify the MCU of events during the data transfer process , RCC global interrupt running on High Speed Clock (HSE) with Low speed Clock (LSE). Used interrupt are also on SPI1 and USART2, which can trigger an interrupt service routine (ISR) to handle specific events related to SPI or USART communication, such as data transmission or reception, errors, or buffer empty/full conditions.

For SPI ensuring communication between the STM32 and RF module, is SPI1 settled in Full-Duplex Master Mode, with hardware NSS signal disabled. It is using

Motorola frame format with data size of 8 bits and MSB first. Prescaler used is 16, with baud rate 3 Mbits/s.

USART2 is utilized for receiving commands from PC users and capturing incoming data from satellite, which can subsequently be visualized through a serial link. This communication interface enables the microcontroller to establish a connection with external devices, such as a PC or a satellite, to facilitate data exchange and enable the visualization or processing of the received information. USART2 mode is Asynchronous mode, which supports variable data lengths, parity bits, and stop bits, providing flexibility for different communication protocols and data formats. Baud rate used for Ground station is 115 200 Bits/s with 8 Bits word length with no parity and 1 stop bit.

6.2 Function

The functional part of the Ground station is structured into various components. Within the private typedefs, several enumerations are defined to enhance the clarity and organization of the code. These include Task_t, representing the tasks that need to be executed; Response_t, defining the response states of Failure or Success; state_t, corresponding to the state values of High or Low; and response_type_t, handling the types of response variables.

Private variables which are handlers for shpi1 - SPI1 peripheral, huart2 handler for USART2 peripheral. The "hdma_usart2_rx" represents the DMA handle for USART2 RX, which is responsible for handling data reception. The "TaskToRun" variable indicates the specific task that needs to be executed. The "RxBuff" is a receive buffer used for UART communication, while the "SWstate" variable keeps track of the current state (LOW or HIGH) of a switch. Additionally, there are other variables utilized in the LoRa functionality, serving various purposes within the system.
Then, there are used several function prototypes for inzialization of DMA, GPIO, USART2, SPI1, system clock Config, which is configuring clock and several task functions and helper function _write().

In the main() function, the system initialization takes place, including the initialization of the HAL library and peripheral devices. The configuration and initialization of the LoRa module are also performed here. The main loop is then entered, where the code waits for UART commands and executes the corresponding tasks.

The HAL_UARTEx_RxEventCallback() function is triggered when a command is received, setting the TaskToRun variable based on the received command. Inside the main loop, the code checks the TaskToRun variable and executes the corresponding task function. This loop continues indefinitely. The HAL_UARTEx_RxEventCallback() function handles UART receive events, determining the received command, storing it in the RxBuffrt buffer, and restarting UART reception to await the next command.
It is triggered when data is received by the UART module, specifically USART2. Upon receiving a command from the PC, the function checks the content of the received buffer

(RxBuffer) for specific command patterns (Command1 to Command4) using the strstr function. Depending on the detected command, the corresponding task is set to be executed in the main loop by assigning the appropriate value to the TaskTRun variable. Additionally, if the received command indicates a state change (e.g., "HIGH" or "LOW") for Task 3 and Task 4, the SWstate variable is updated accordingly. If no predefined commands match, the program enters the IDLE state. Finally, the function restarts the receive process, preparing to receive further commands, and disables the appropriate DMA interrupt to keep the interrupt service routine (ISR) short.

In addition to the main functions described earlier, there are a couple of additional functions within the codebase. One of them is the IDLETask() function, which is called when no specific task is selected, indicating that the system is in an idle state. This function handles any necessary actions or operations during this idle period.Another function is _write(), which serves as a helper function in the code. Its purpose is to redirect the standard output, commonly used for functions like printf, to the UART interface. By doing so, it enables communication through the designated serial interface, allowing data to be transmitted and received.

Overall, the code's main focus is on configuring and setting up the microcontroller peripherals, initializing the LoRa module, and continuously monitoring for incoming UART commands. It leverages the UART interface to facilitate communication with a PC, enabling command-based interactions, while the LoRa module is employed for communication with other devices.

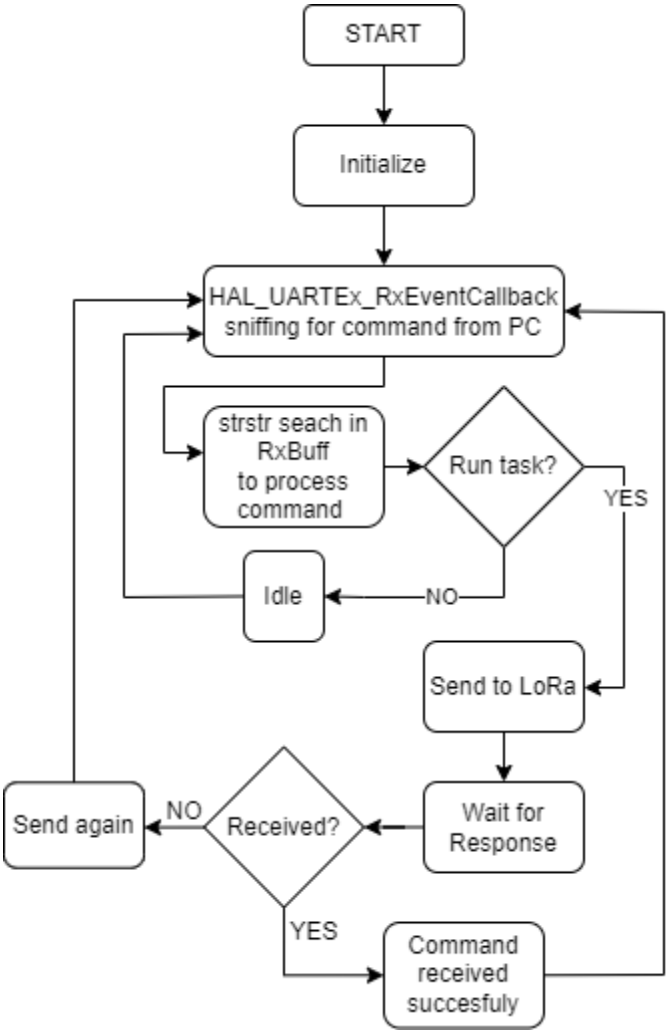

Figure 24: Flow diagram of Ground station

6.3 Code execution order

The program commences by undertakin the initialization process for the microcontroller and its peripheral configurations. This contain setting up the system clock, GPIO pins, UART (Universal Asynchronous Receiver-Transmitter), SPI (Serial Peripheral Interface), and DMA (Direct Memory Access). Furthermore, the LoRa (Long-Range) module, specifically the SX1278, is initialized with meticulous parameterization encompassing frequency, power, spreading factor, bandwidth, coding rate, cyclic redundancy check (CRC), and packet length.

Progressing to the command reception phase, the program enters an infinite loop, where itt is awaiting user commands. These commands are acquired through the UART interface, employing DMA for seamless, non-blocking reception. Upon receiving a command, an interrupt is instantaneously triggered, facilitating the storage of the command within the designated RxBuff array. Subsequently, the received command undergoes scan as it is compared against a set of predefined commands (Command_1, Command_2, Command_3, and Command_4) via string comparison.

In the subseqent task execution stage, the program dynamically selects the appropriate task to execute based on the received command. Should Command_1 be received, Task 1 function is invoked, while Command_2 triggers the execution of Task 2 function. Similarly, Command_3 prompts the initiation of Task 3 function, and Command_4 leads to the execution of Task 4 function. If none of the predefined commands correspond, the program transitt into the IDLE state, ready to perform idle tasks or await fresh commands.

The execution of tasks involves performing specific sequences of operations for Task 1, Task 2, Task 3, and Task 4. Each task follows a sequential order of steps to be carried out. Upon calling Task_1, a message is printed, denoting the invocation of Task 1. Subsequently, the SX1278 module is employed to initialize a LoRa transmission. The Task_1 command is then passed to to all connected slave devices within the LoRa network (satellite). After a designated delay, a comprehensive package containing the command is transmitted via LoRa using the SX1278 module. Task 2, Task 3, and Task 4 follow a similar execution pattern, involving message printing, command dissemination to slave devices, state manipulation based on the command, and subsequent transmission via LoRa.IDLE Task.

In scenarios where the received command fails to match any predefined commands, the program run transitions into the IDLE state. This prompts the execution of the IDLE_Task function, making it LoRa module goto idle state. This IDLE state is embedded within a continuous loop, enabling the program to perpetually iterate. Within this loop, periodic heartbeat messages are dispatched to the UART interface, serving as an indication of the program's operational status. Program consistently monitors for incoming commands, promptly executing the corresponding tasks upon their detection.

7. POCKETQUBE FW

7.1 Introduction

The following part represents an integral component of a satellite system, specifically designed for communication and task execution. This side was also developed in CubeMX and Cubde IDE. Whole program is written in C language and HAL libraries are also used.

The hardware board features dedicated programming pins that allow for easy programming of the microcontroller. These pins can be conveniently connected to an external programmer, such as the ST-LINK included in the Nucleo development board.By utilizing these programming pins, developers have the flexibility to update the firmware on the microcontroller without the need for additional hardware modifications. The ST-LINK, or a compatible programmer, can establish a connection with the board and transfer the compiled code to the microcontroller for execution.This programming capability simplifies the development and debugging process, as it enables quick and efficient firmware updates, ensuring that the microcontroller is running the latest version of the code. Exact pins for uploading code on board are SWCLK, GND, SWDIO, NRST and sensing pin for voltage. This can be found in Appendix A.

Developed for the satellite side, this program leverages LoRa (Long Range) communication, ADC (Analog-to-Digital Converter) measurements, and EEPROM (Electrically Erasable Programmable Read-Only Memory) data reading functionalities. Through the seamless integration of these capabilities, the program facilitates efficient communication with a ground station while enabling the execution of various predefined tasks.

Program is establishing a communication channel between satellite and ground station using the LoRa module. It initializes and configures module with specific parameters, allowing bidirectional communication.

In this code configuration, the system utilizes the System Tick Timer as its time base. The System Tick Timer is timekeeping and synchronizating the program. By relying on this timer, the code can accurately measure time intervals and synchronize various tasks. Operating at a consistent frequency, the System Tick Timer generates periodic interrupts by Time base: system tick timer interrupt, allowing the program to maintain a reliable and synchronized time reference. For Clock configuration, this core is running on 16 MHz external crystal connected on RCC_OSC_IN (PIN PD0) and RCC_OSC_OUT (PIN PD1). Low speed clock is disabled in this application and not used.

For conversion of voltages measured on pins, is ADC1 mode used, which is 12-bit successive approximation analog-to-digital converter module that allows the microcontroller to convert analog signals into digital values. STM32F103RBT6 is corresponding with 15 channels of ADC converter, from which are 8 used.

The STM32F103RBT6 microcontroller supports the I2C (Inter-Integrated Circuit) communication protocol, which is widely used for connecting multiple devices on a bus and enabling communication between a master device and one or more slave devices. In this particular setup, an EEPROM is connected to this communication bus.The I2C connection in this configuration operates in Standard mode with a fast mode clock speed of 1 MHz. The I2C1_SCL and I2C1_SDA pins are used for establising the I2C connection, and they are mapped to pins PB6 and PB7, respectively. Using this I2C interface, the microcontroller can send commands to the connected slave device, read data from it, and receive responses. This allows for communication and interaction between the microcontroller and the EEPROM, enabling data storage and retrieval.

To facilitate testing and monitoring of satellite communication, USART1 mode has been implemented on the board. This mode enables the observation of received and transmitted data. The USART1 is connected to a debug pin row for easy access.In this configuration, the USART1 mode utilizes pin PA10 for RX (receive) and pin PA9 for TX (transmit). The USART operates in asynchronous mode with a Baud Rate of 115,200 Bits/s. The data format consists of 8 bits with 1 stop bit. The USART1 mode supports both receive and transmit operations, allowing for bidirectional communication. This setup provides a convenient way to monitor the satellite's communication activity, enabling the observation of incoming and outgoing data in real-time.

The most important peripheral on the board is SPI2, which communicates with the LoRa module. It utilizes several pins for this purpose, including MOSI (PB15), MISO (PB14), SCK (PB13), NSS (PB12), RESET (PB1), and the DIO0 interrupt pin (PB8). SPI2 plays a crucial role in enabling seamless data exchange between the microcontroller and the LoRa module. MOSI transmits data from the microcontroller to the module, while MISO receives data from the module. SCK synchronizes the data transfer, and NSS activates the LoRa module for communication. The RESET pin allows for resetting the LoRa module, ensuring proper initialization. The DIO0 interrupt pin serves as a signal line, triggering the microcontroller when specific events occur on the LoRa module.

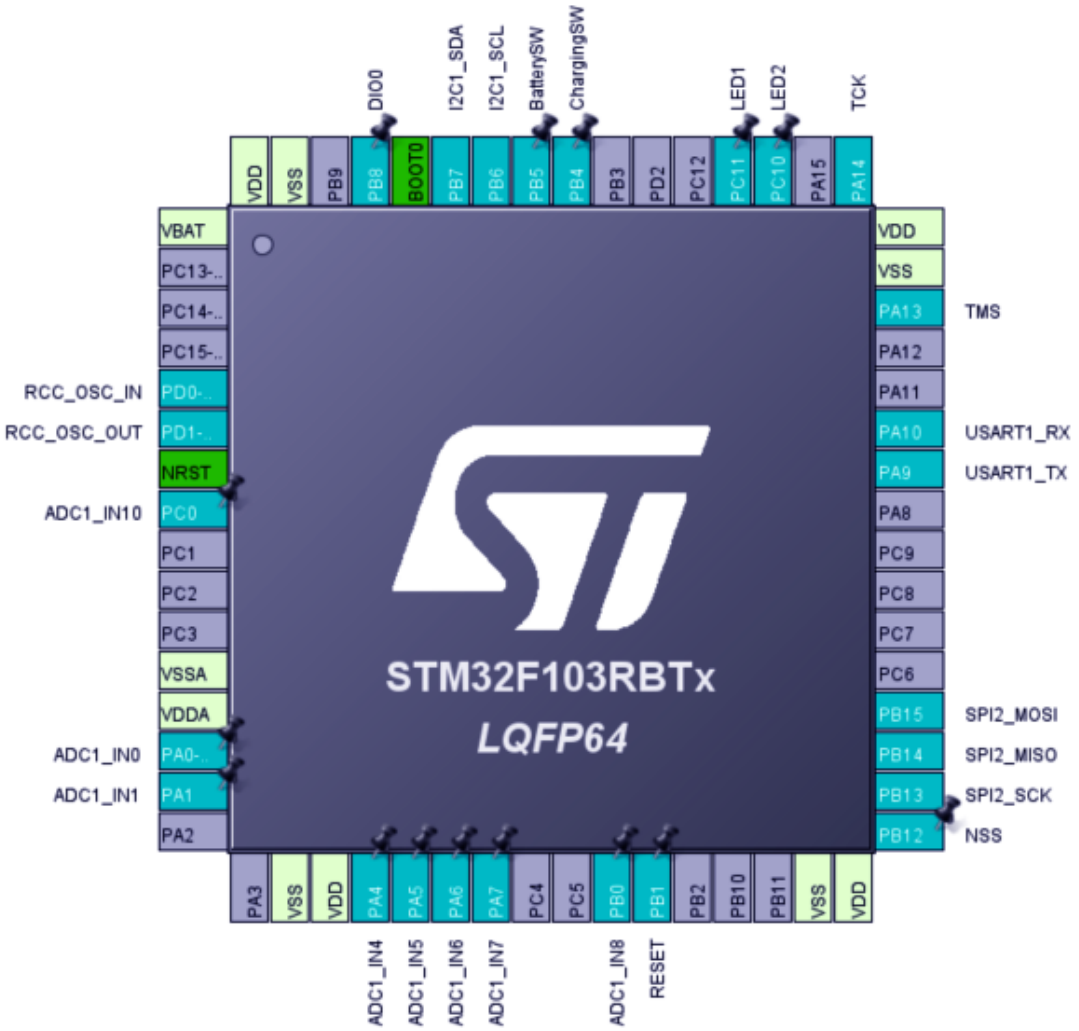

Figure 25: Pin configuration on PocketQube main STM32

7.2 Function

The main function in this code snippet is responsible for receiving data on a LoRa module and subsequently processing it based on the required evaluation.

At the beginning system incorporates several typedefs to manage responses and states effectively. Task_t is used to define the different tasks that the system can perform, allowing for easy identification and organization. Response_t is utilized to define the response status of a task, distinguishing between success and failure outcomes. State_t, on the other hand, is employed to define the state of a signal, offering options such as LOW or HIGH to indicate the current condition. Additionally, the response type typedef serves as an alias for uint8_t, enabling convenient data handling and manipulation related to response types. By utilizing these typedefs, the system ensures clear and consistent representation of task statuses, response outcomes, and signal states, enhancing overall system functionality and maintainability.

At beginning, there are settled RxBuffer_size, which sets the size of the receive buffer to 200 bytes. Following that, there are macro definitions for different commands such as ReadADC, ReadFromEEPROM, ChargeSW, and BatterySW. The ThisNodeAddress macro specifies the address of the current node.

The EEPROM_writing_time macro determines the time interval for writing to the EEPROM, which can be set accordingly to application, currently is set to 10 minute. That means, that ADC values are written to EEPROM every 10 minutes and can be changed with recalculating the time. The EEPROM_ADDR macro defines the address of the EEPROM, set to 0xA0. Additionally, the PAGE_SIZE macro specifies the page size for EEPROM operations, set to 128 bytes, and the PAGE_NUM macro denotes the total number of pages in the EEPROM, set to 512 pages. Accordingly to CubeMX IDE, there was generated HAL handlers for hadc1, hic2c1, hspi2 and huart1.

Several private variables are defined to handle different peripherals, manage the LoRa modem configuration, store data in buffers, handle tasks, and track timing. Among these variables, noteworthy ones include SX1278_hw and SX1278, which are used for configuring the LoRa modem, RxBuffer for storing received data, TasktoRun for managing tasks, and last_eeprom_write_time for keeping track of the most recent EEPROM write operation.

7.3 Execution order

The program begins with the main function, which serves as the entry point of the application. In this function, various initialization functions are called to set up the system clock, GPIO pins, SPI, UART, ADC, and I2C interfaces. These initializations ensure that the necessary hardware resources are properly configured for the program's operation. Once the hardware initialization is complete, the function for initialize of LoRa RX modem function is invoked. This function initializes the LoRa library modem for receiving data. It configures parameters such as frequency, bandwidth, spreading factor, and coding rate to establish communication settings.

To ensure a clean slate, the EEPROM memory is cleared, and a default message that EEPROM is not used. This message serves as an indication that the EEPROM is currently not utilized by the program. The program then enters the main while loop, which acts as the primary execution loop, running indefinitely until interrupted. Within this loop, a delay of 1000 milliseconds (1 second) is introduced using the HAL_Delay function. This delay serves as a timing mechanism to control the execution frequency of the loop. Next, the Listen_On_LoRa function is called to check if there is any incoming data on the LoRa modem. This function listens for incoming messages and retrieves them if available. If data is received, it is stored in the RxBuffer array for further processing. After checking for incoming data, the program examines the value of the TaskToRun variable to determine which task should be executed next. This variable acts as a control mechanism for task selection and sequencing. Based on its value, the corresponding task

function is called. The program incorporates four distinct task functions for Task1 to Task4. Each task function carries out specific operations or calculations as required by the application. The execution of a particular task is determined by the value assigned to TaskToRun at a given moment. If the value of TasktoRun indicates IDLE, the program invokes the IDLETask function. This task is typically used when there are no specific operations to be performed, allowing the program to remain in an idle state until a new task is triggered.

Upon completing the execution of a task, the program checks the last_eeprom_write_time variable to determine if it is time to write data to the EEPROM. This variable represents the elapsed time since the last write operation to the EEPROM. If the elapsed time since the last EEPROM write is equal to or greater than the predefined EEPROM writing time (e.g., 10 minutes), the program proceeds with reading ADC values from connected sensors or inputs. The obtained data is then formatted into a suitable string representation and subsequently written to the EEPROM memory for storage.

After the EEPROM write operation or if the elapsed time condition is not met, the main while loop continues, and the entire process repeats. This ensures that the program consistently listens for incoming data, executes tasks as required, and handles the periodic writing of data to the EEPROM. In summary, the main function establishes the program flow by initializing hardware, setting up the LoRa modem, listening for data, executing tasks based on the TasktoRun value, and performing periodic EEPROM writes.

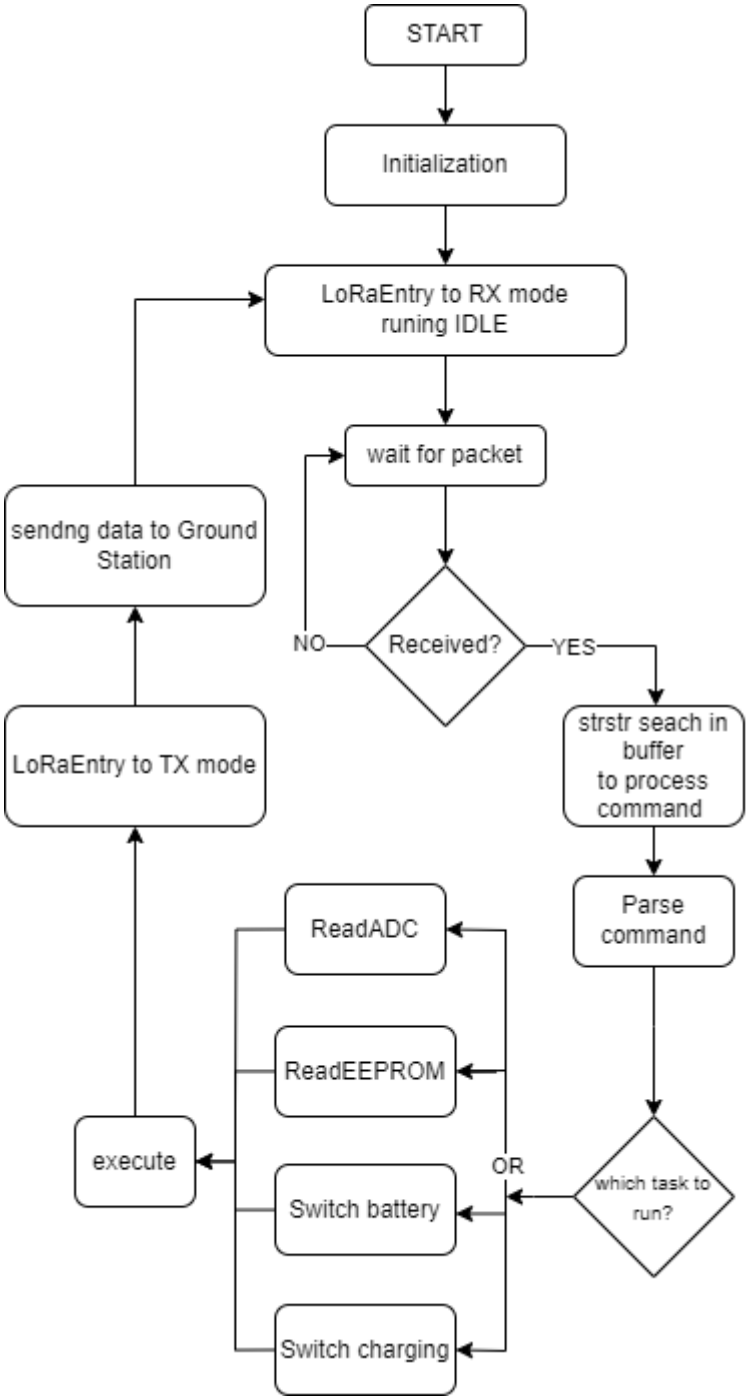

Figure 26: State diagram of PocketQube model

8. REAL MODEL AND TESTING

On the next Figures, model of PocketQube and Groundstation is presented. PocketQube is the same dimensions as in technical drawings in Appendix J. Whole construction is screwed together with M2 screws. Also demonstrative model of "deployer" tray was included.

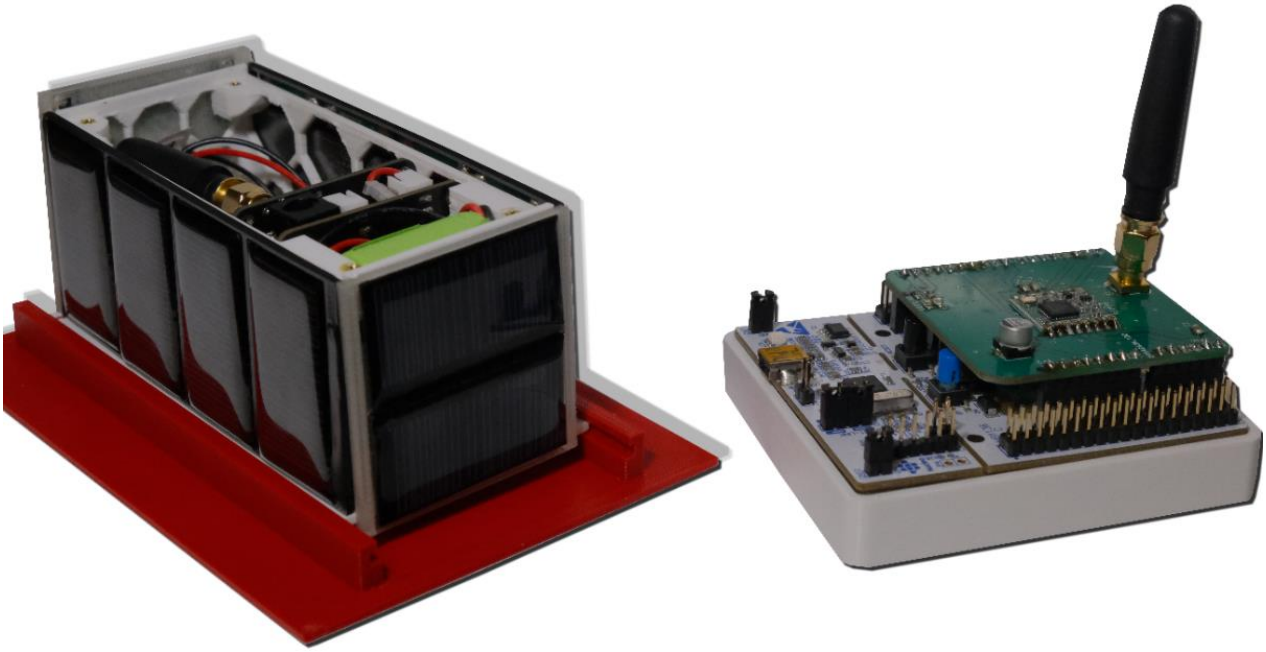

Figure 27: PocketQube model and Ground station

Figure 28: Detail on the PocketQube Electronics and inner structure

The following figures illustrate examples of communication scenarios. In the first example, a ReadADC command is sent from the GroundStation to the Satellite. The Satellite receives this command, prints the ADC values to the serial communication on its side, and transmits them over LoRa back to the GroundStation. The command for reading the ADC values is organized as follows:

Voltages: PV1, PV2, PV3, PV4, PV5, Charging current, Discharging current, Battery Voltage

In this example, the GroundStation initiates the communication by requesting the ADC values from the Satellite. The Satellite receives the command, retrieves the ADC values for various voltages (PV1 to PV5), as well as the charging current, discharging current, and battery voltage. It then prints these values to the serial communication for local observation. Additionally, the Satellite transmits the ADC values over the LoRa network, allowing the GroundStation to receive and process the data for further analysis or display. Hercules Setup utility was the software employed to facilitate the display of communication between the Satellite and GroundStation. This utility offers a user-friendly graphical interface (GUI) that enables seamless transmission and reception of data via COM ports. With its intuitive features, Hercules

Setup utility proved to be an effective tool for visualizing and managing the data exchange process between the two systems.

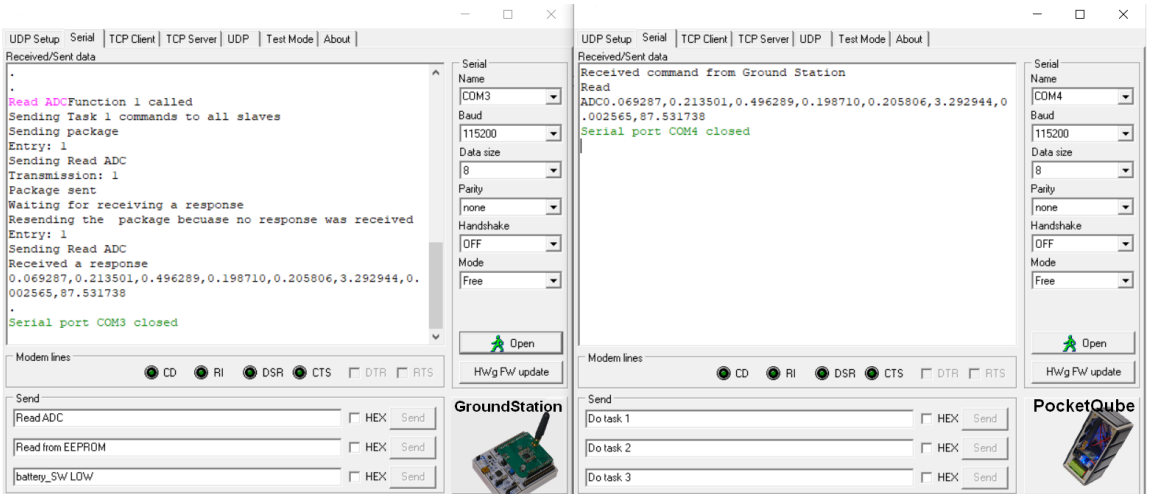

Figure 29: Communication of reading ADC from PocketQube

In the following example, data retrieval from the EEPROM is demonstrated by sending the command ReadFromEEPROM This command triggers the satellite to access the stored data in the EEPROM, which is regularly written at specified intervals. Once the data is read, the EEPROM is subsequently erased, preparing it for the next cycle of data storage. This process ensures a continuous flow of updated information from the EEPROM, enabling efficient data management and utilization.

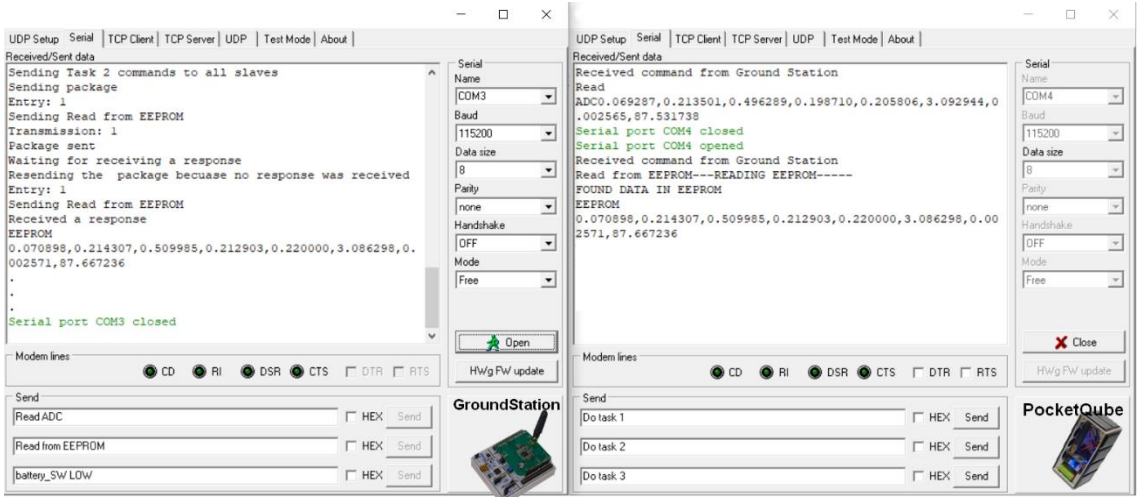

Figure 30: Receiving data stored in EEPROM

The last example involves sending a straightforward command to set a pin to either logical "1" or logical "0". This action serves as a trigger to activate or deactivate the charging path or battery path. By manipulating the pin's logic level, the desired power pathway can be controlled effectively. This functionality enables efficient

management of the charging and discharging processes, allowing for precise control over power flow within the system.

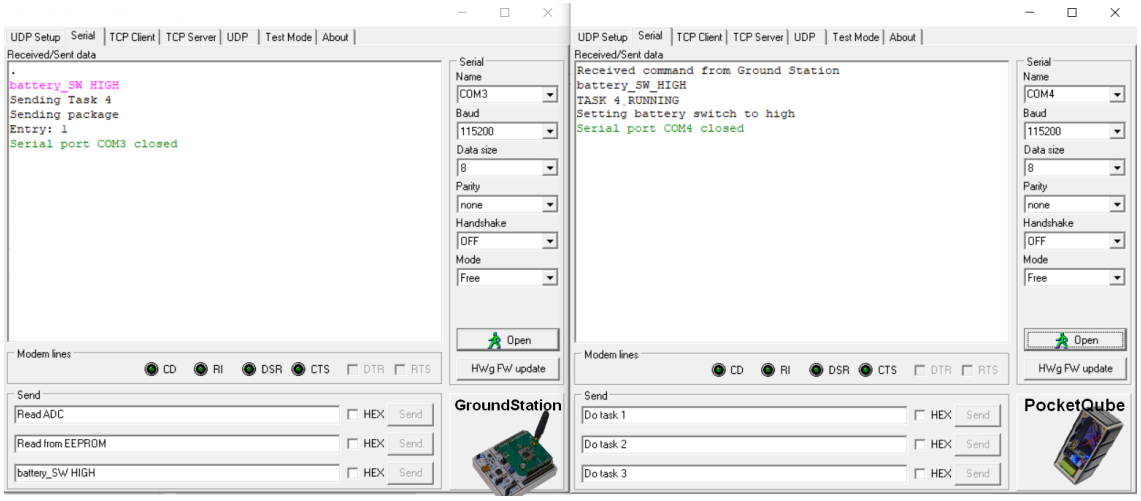

Figure 31: Example of sending command to set SW of battery/charging to LOW or HIGH

9. DISCUSSION

The primary objective of this thesis was to formulate a proposition for an educational-oriented small nanosatellite in the PocketQube format. The initial system design and subsequent implementation were carried out for the power supply system, the main on-board computer, and the communication component. Simultaneously, a ground station was developed as part of the system, incorporating the same communication scheme as in the PocketQube. The ground station serves as a communication channel between the PC and the system via a COM interface.

At the outset of this thesis, a comprehensive exploration was undertaken to examine the present issues and challenges associated with PocketQube format satellites. These encompassed factors like their compact size, constrained power resources, necessitating a thoughtful selection of power management techniques and optimal energy utilization to guarantee the satellite's successful operation. Additionally, considerations were given to the limited payload capacity and to the most important module of satellite - communication constraints faced by such satellites. Due to these factors, the decision was made to utilize an STM32 microcontroller and an RFM96W Lora module for communication between the satellite and the ground station. In Chapter 4.2.1, a concise overview of LoRa was provided, including the selection of a communication module and a clear description of its parameters, specifically focusing on its chirp spread spectrum functionality. It has been demonstrated that communication with the LoRa module is achievable, with the link budget proving to be favorable and feasible in this specific configuration on the PocketQube. As proof, the successful implementation of LoRa communication in orbit [32] represents a significant step forward in space technology and highlights the ambitious prospects for the future of space missions.

I conducted thorough research on various components of this type of satellite, including the selection of MCUs (Microcontrollers), communication modules, photovoltaic panels, power supply management ICs and batteries. Also the power budget was described for model situation and real in space situation. Schematics of this modules incorporating were developed and then converted to PCB layout in PQ60 format. This system incorporated to two main blocks of power supply on one PCB and communication module with MCU on second PCB, which are stackable via row pin header, which is providing a future possibility in further development. Firmware was developed for this microcontroller, containing all peripherals needed for smooth for smooth functioning such as SPI for establishing connectivity between LoRa module, I2C connectivity for accessing memory and several GPIO pins for additional.

Communication is running in 433 MHz frequency with LoRa modulation between Ground station and satellite model. It is controlled with command for Reading real time ADC values from satallite, reading EEPROM which is storing data periodically and

erasing its content when sending it to Ground station and possibility of switching on or off powering nodes on satellite.

Communication were tested with commanding the satellite as can be seen in Figures 29-31, for proposed commands.

The mechanical construction successfully incorporated all the required modules while adhering to the size specifications for a 2p structure. The structure encompasses a fully 3D printed frame with panels on either side, specifically designed to accommodate photovoltaic panels. For this educational application, PLA material was utilized for the printing process. The model exhibits versatility and can be easily customized for future applications. Employing 3D printed material for the frame offers a cost-effective solution. However, in the future, integrating FR4 panels, such as 1mm thick ones, to encompass the entire satellite and integrating solar panels onto them would be an even more optimal choice.

The educational satellite offers practical demonstrations of utilizing the LoRa communication layer, addressing challenges such as limited power resources. It facilitates extensive testing with customizable parameters. Going forward, this initiative serves as a foundation for expanding subsystems, conducting payload experiments, enhancing the satellite's functionalities, and designing specialized LoRa module antennas. Ultimately, this satellite serves as an invaluable educational tool, offering students a hands-on experience and fostering their learning.

LITERATURE

[1] Puig-Suari, J., Turner, C., & Ahlgren, W. (n.d.). Development of the standard CubeSat deployer and a CubeSat class PicoSatellite. In 2001 IEEE Aerospace Conference Proceedings [online]. [cit. 2022-10-25]. Available at: https://doi.org/10.1109/aero.2001.931726

[2] POVALAČ, A. Nanosatellite Design and Electronics. Brno: Brno University of Technology, Faculty of electrical engineering and communications, 2021.

[3] Bouwmeester, J., Radu, S., Uludag, M. S., Chronas, N., Speretta, S., Menicucci, A., & Gill, E. K. A. (2020). Utility and constraints of PocketQubes. CEAS Space Journal, 12(4), 573-586 [online]. [cit. 2022-10-25]. Available at: https://doi.org/10.1007/s12567-020-00300-0

[4] R. Twiggs, Making it Small, in Proceedings of the CubeSat Developers Workshop (California Polytechnic State University, San Luis Obispo, 2009). [online]. [cit. 2022-10-25]. Available at: https://www.klofas.com/comprehensive.html

[5] Azami, M.H.b.; Orger, N.C.; Schulz, V.H.; Oshiro, T.; Cho, M. Earth Observation Mission of a 6U CubeSat with a 5-Meter Resolution for Wildfire Image Classification Using Convolution Neural Network Approach. Remote Sens. 2022, 14, 1874. [online]. [cit. 2022-10-25]. Available at: https://doi.org/10.3390/rs14081874

[6] Fossa Systems And Exolaunch Announce The Launch Of Eight Pocketqube Satellites In Q4 2021 [online]. [cit. 2022-10-25]. Available at: https://fossa.systems/fossa-systems-and-exolaunch-announce-the-launch-of-eight-pocketqube-satellites-in-q4-2021-2/

[7] Radu, S., Uludag, S., Speretta, S., Bouwmeester, J., Gill, E., & Chronas Foteinakis, N. (2018). Delfi-PQ: The first pocketqube of Delft University of Technology [online]. [cit. 2022-10-25]. Available at: http://resolver.tudelft.nl/uuid:e9129c1d-273f-4f93-be93-05d5f7cc4ce8

[8] CubeSat Design Specification (1U – 12U) REV 14.1 CP-CDS-R14.1 [online]. [cit. 2022-10-25]. Available at: https://static1.squarespace.com/static/5418c831e4b0fa4ecac1bacd/t/62193b7fc9e72e0053f00910/1645820809779/CDS+REV14_1+2022-02-09.pdf

[9] Park, S. J., Lee, J. E., Park, J., Lee, N.-K., Son, Y., & Park, S.-H. (2021). High-temperature 3D printing of polyetheretherketone products: Perspective on industrial manufacturing applications of super engineering plastics. Elsevier BV. [online]. [cit. 2022-10-25]. Available at: https://doi.org/10.1016/j.matdes.2021.110163

[10] Arif, M. F., Kumar, S., Varadarajan, K. M., & Cantwell, W. J. (2018). Performance of biocompatible PEEK processed by fused deposition additive manufacturing. Elsevier BV. [online]. [cit. 2022-10-28]. Available at: doi.org/10.1016/j.matdes.2018.03.015

[11] Albapod Interface Control Document [online]. [cit. 2022-10-28]. Available at: https://static1.squarespace.com/static/53d7dcdce4b07a1cdbbc08a4/t/607eb95a8453342db546143f/1618917746906/AlbaPod+ICD+v.02+

[12] NuttX RTOS for Satellite control [online]. [cit. 2022-11-10]. Available at: https://nuttx.events/wp-content/uploads/2019/11/balzano_nx2019.pdf

[13] Nielsen, J. D., & Larsen, J. A. (2011). A decentralized design philosophy for satellites. [online]. [cit. 2022-11-10]. Available at: https://doi.org/10.1109/rast.2011.5966896

[14] Atem de Carvalho, R., Estela, J., & Langer, M. (Ed.). (2020). Nanosatellites. Wiley. [online]. [cit. 2022-11-10]. Dostupné z: https://doi.org/10.1002/9781119042044

[15] The Things Network. Lora World Record Broken: 832km/517mi Using 25 mw. [online]. [cit. 2022-11-13]. Available at: https://www.thethingsnetwork.org/article/lorawan-world-record-broken-twice-insingle-experiment-1

[16] Lacuna Space. Lacuna Space Achieves Major Milestone for LoRa in Space. [online]. [cit. 2022-11-18]. Available at:: https://lacuna.space/lacunaspace-achieves-major-milestone-for-lora-in-space/

[17] Fossa Systems. LoRa Ground Station Development Kit. [online]. [cit. 2022-11-18]. Available at: https://fossa.systems/product/lora-groundstation-development-kit/

[18] Fernandez, L., Ruiz-De-Azua, J. A., Calveras, A., & Camps, A. (2020). Assessing LoRa for Satellite-to-Earth Communications Considering the Impact of Ionospheric Scintillation. Institute of Electrical and Electronics Engineers (IEEE) . [online]. [cit. 2022-11-18]. Available at: https://doi.org/10.1109/access.2020.3022433

[19] Al-Khazzar, Akram & Hashim, Emad. (2015). Temperature Effect on Power Drop of Different Photovoltaic Modules. . [online]. [cit. 2022-11-18]. Available at: https://www.researchgate.net/publication/284970252_Temperature_Effect_on_Power_Drop_of_Different_Photovoltaic_Modules

[20] Building and flying the world's smallest Spacecraft Attitude Determination and Control System . [online]. [cit. 2022-11-18]. Available at: http://www.albaorbital.com/new-blog/2020/11/24/building-and-flying-the-worlds-smallest-spacecraft-attitude-determination-and-control-system

[21] RF Transceiver Module RFM9xW (datatsheet) [online]. [cit. 2022-11-18]. Available at: https://www.hoperf.com/modules/lora/RFM98.html

[22] Mainstream Performance line, Arm Cortex-M3 MCU with 64 Kbytes of Flash memory, 72 MHz CPU, motor control, USB and CAN (datasheet) [online]. [cit. 2022-11-18]. Available at: https://www.st.com/en/microcontrollers-microprocessors/stm32f103c8.html#documentation

[23] Ultralow Power RS485 Transceiver with Shutdown LTC1418F (datasheet) [online]. [cit. 2022-12-10]. Available at: https://www.analog.com/media/en/technical-documentation/data-sheets/1481fa.pdf

[24] Microchip Technology Inc. 24AA512/24LC512/ 24FC512 (24XX512*) EEPROM [online]. [cit. 2022-12-10]. Available at: https://www.tme.eu/Document/a1c661e4ce129aa1aa814866fd359d72/24lc512.pdf
[25] Linear current sensing chip ACS712 [online]. [cit. 2022-12-10]. Available at: https://www.sparkfun.com/datasheets/BreakoutBoards/0712.pdf
[26] Mono/polycrystalline solar panel battery module [online]. [cit. 2022-12-10]. Available at: https://www.aliexpress.com/item/4001240640418.html
[27] Github repository of LoRa SX1278 communication library [online]. [cit. 2022-12-10]. Available at: https://github.com/wdomski/SX1278
[28] Graf vypustených nanosatelitov [online]. [cit. 2022-12-19]. Available at: https://www.nanosats.eu/
[29] AlbaOrbital deployer [online]. [cit. 2022-12-19]. Available at: http://www.satnews.com/story.php?number=1076719166
[30] AlbaOrbital PocketQube [online]. [cit. 2022-12-19]. Available at: OBC http://www.albaorbital.com/hardware/on-board-computer
[31] AlbaOrbital PocketQube kit [online]. [cit. 2022-12-19]. Available at: http://www.albaorbital.com/hardware/pocketqube-kit
[32] FossaSat-1 documentation [online]. [cited 2023-03-14] Available at: https://github.com/FOSSASystems/FOSSASAT-1
[33] Datasheet for MSP430 MCU [online]. [cited 2023-03-14] https://www.alldatasheet.com/datasheet-pdf/pdf/465689/TI1/MSP430.html
[34] Datasheet for PIC32MX [online]. [cited 2023-03-14] Available at: https://ww1.microchip.com/downloads/en/DeviceDoc/PIC32MX_Datasheet_v2_61143B.pdf
[35] Research on low power applications for Atmel 328p, Datasheet for MSP430 MCU [online]. [cited 2023-03-14] Available at: http://www.elektromys.eu/clanky/avr_lowpower/clanek.html
[36] All About LoRa and LoRaWAN, LoRa physical layer solutions. [online]. [cited 2023-03-20] Available at: http://www.sghoslya.com/p/lora-is-chirp-spread-spectrum.html
[37] Recommendation T/R 61-02 (Chester 1990, Nicosia 1994, The Hague 01, Vilnius 04) (HAREC), [online]. [cited 2023-03-20] Available at: http://www.crk.cz/HARECC
[38] Bäumker, E., Miguel Garcia, A., & Woias, P. (2019). Minimizing power consumption of LoRa® and LoRaWAN for low-power wireless sensor nodes. In Journal of Physics: Conference Series (Vol. 1407, Issue 1, p. 012092). IOP Publishing. Availabe at: https://doi.org/10.1088/1742-6596/1407/1/012092
[38] Datasheet for MAX481 / MAX483 / MAX485 / MAX487 – MAX491 / MAX1487: Low-Power, Slew-Rate-Limited RS-485 / RS-422 Transceivers [online]. [cited 2023-03-20] Available at: https://www.tme.eu/Document/249edd92415e56b4862d1dc20b9d3c0a/MAX1487-MAX491-DTE.pdf

[40] Datasheet ISL3179E, ISL3180E RS485 driver [online]. [cited 2023-03-20] Available at: https://www.tme.eu/Document/71c5480207b603aeb010be37e8a35bc1/ISL3179EFBZ.pdf
[41] Datasheet for SP3483 3.3V Low Power Slew Rate LimitedHalf-Duplex RS-485 Transceiver [online]. [cited 2023-03-20] Available at: https://www.tme.eu/Document/bb229d8a10234eccdd9d0bd35b9b2c32/sp3483.pdf
[42] Pumpkin CubeSat Kits [online]. [cited 2023-05-20] Available at: https://www.cubesatshop.com/product/pumpkin-cubesat-kits/
[43] GomSpace X-Band Transceiver, [online]. [cited 2023-05-15] Available at: https://gomspace.com/shop/subsystems/communication-systems/default.aspx
[44] Lora module RF-LORA-868-SO-DTE datasheet, [online]. [cited 2023-05-15] Available at: https://www.tme.eu/Document/72355fcf885bca99d5f10d8cd1ed2070/RF-LORA-868-SO-DTE.pdf
[45] Lora module rc-wle5-868 datasheet, , [online]. [cited 2023-05-01] Available at: https://www.tme.eu/Document/e5e575e4ee9363bd6a49ac45a9e188c8/rc-wle5-868.pdf
[46] Lora module XTR-8LR-ENC datasheet, [online]. [cited 2023-05-01] Available at: https://www.tme.eu/Document/011b00641e551e3acecb73babbc4d96b/XTR-8LR-ENC.pdf
[47] ACS37010 datasheet, [online]. [cited 2023-05-15] Available at: https://cz.mouser.com/datasheet/2/1115/ACS37010_Datasheet-3136917.pdf
[48] MCS1806GS datasheet [online]. [cited 2023-05-01] Available at: https://cz.mouser.com/datasheet/2/277/MCS1806GS-3073842.pdfCT452
[49] CT452 datasheet, [online]. [cited 2023-05-01] Available at: https://cz.mouser.com/pdfDocs/CT452-Data-Sheet-Rev02.pdf
[50] LM1117 3v3 linear regulator with low dropout datasheet , [online]. [cited 2023-05-01] Available at: https://www.ti.com/lit/ds/symlink/lm1117.pdf
[51] Datasheet Antenna for 433MHz, model: 433M-ANT401 [online]. [cited 2023-05-01] Available at: https://www.tme.eu/Document/822a8e330ede636bd02fa33494d22f83/433M-ANT401.pdf
[52] Alba orbital Solar panels for PQ - Solar Panels 1p Set (QTY 5) Datasheet [online]. [cited 2023-05-01] Available at: https://cdn.shopify.com/s/files/1/0284/1072/files/DHV_PDF.pdf?309
[52] Energetic calculations for small spacecrafts, [online]. [cited 2023-05-01] Available at: https://github.com/alanbjohnston/CubeSatSim, https://www.amsat-ea.org/
[53] EEPROM M24C32 i2c memory datasheet, [online]. [cited 2023-05-01] Available at: https://www.st.com/resource/en/datasheet/m24c32-w.pdf

LIST OF APPENDICES

APPENDIX A – SCHEMATIC OF OBC+COM

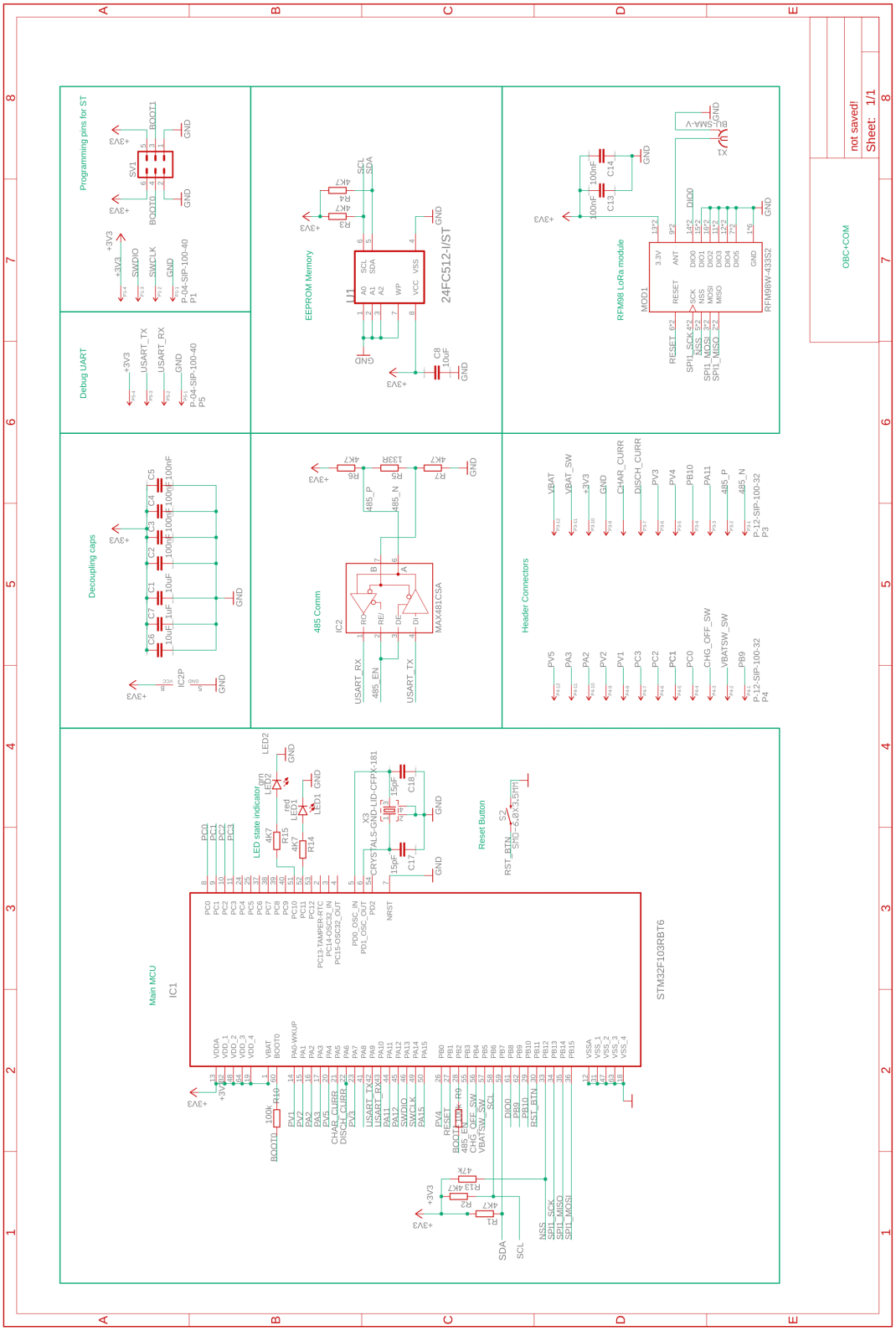

APPENDIX B - OBC+COM PCB (COPPER LAYER)

B1 - TOP SIDE OF PCB – OBC+COM

Scale 1:1 (42mm x 42mm) PCB

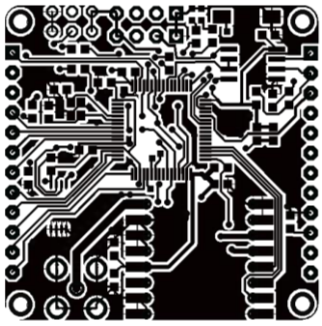

B2 - BOTTOM SIDE OF PCB – OBC+COM

Scale 1:1 (42mm x 42mm) PCB

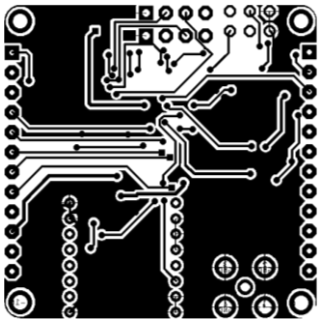

APPENDIX C – COMPONENT PLACEMENT AND BOM – OBC+COM

C1 – COMPONENT PLACEMENT (SCALE 2:1)

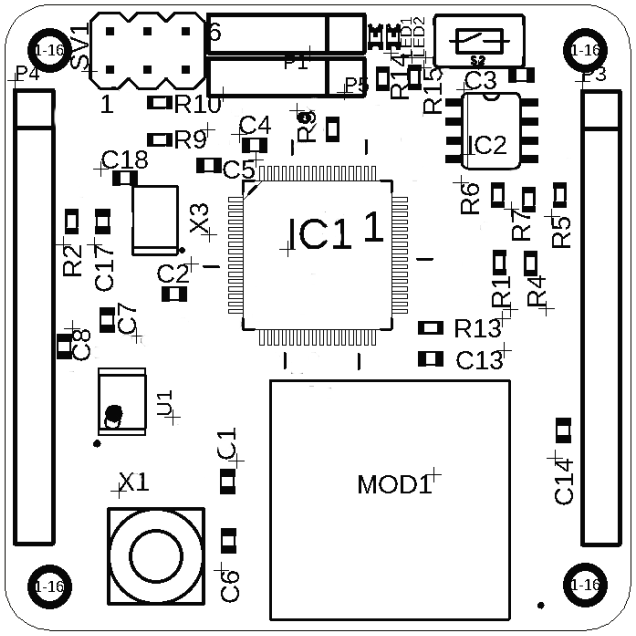

C2 – BOM

Part	Value	Device	Package	Description
C1, C2. C3, C4, C5, C6, C7, C8, C13, C14	100nF	CC0603	C0603	Ceramic capacitor
C17, C18	15pF	CC0603	C0603	Ceramic capacitor
IC2	MAX481CSA	MAX481CSA	SO08	RS485 TRANSEIVER
LED1	red	LEDCHIPLED_0603	CHIPLED_0603	LED
LED2	grn	LEDCHIPLED_0603	CHIPLED_0603	LED
MOD1	RFM98W-433S2	RFM98W-433S2	XCVR_RFM98W-433S2	RFM98W LoRaModule 433MH
P1	P-04-SIP-100-40	P-04-SIP-100-40	SIP-100-04-40	HEADER PLUG PINS
P3	P-12-SIP-100-32	P-12-SIP-100-32	SIP-100-12-32	HEADER PLUG PINS
P4	P-12-SIP-100-32	P-12-SIP-100-32	SIP-100-12-32	HEADER PLUG PINS
P5	P-04-SIP-100-40	P-04-SIP-100-40	SIP-100-04-40	HEADER PLUG PINS

R1, R2, R3, R4, R6, R7	4K7	R-EU_R0603	R0603	Resistor
R5	133R	R-EU_R0603	R0603	Resistor
R9, R10	100k	R-EU_R0603	R0603	Resistor
R13, R14, R15	47k	R-EU_R0603	R0603	Resistor
S2	SMD-6.0X3.5MM	MOMENTARY-SWITCH	SMD_6.0X3.5MM	Momentary Switch SPST
SV1		MA03-2	MA03-2	PIN HEADER
U1	24FC512	EEPROM	MICROCHIP_24FC512-I-ST_0	MCHP-24-AA-FC512-SOIC-TSSOP-8
X1	BU-SMA-V	BU-SMA-V	BU-SMA-V	FEMALE SMA CONNECTOR
X3	16MHz	CRYSTALS-GND-LID-CFPX-181	2.5X2-4-PAD	CRYSTAL

APPENDIX D – SCHEMATIC - EPS

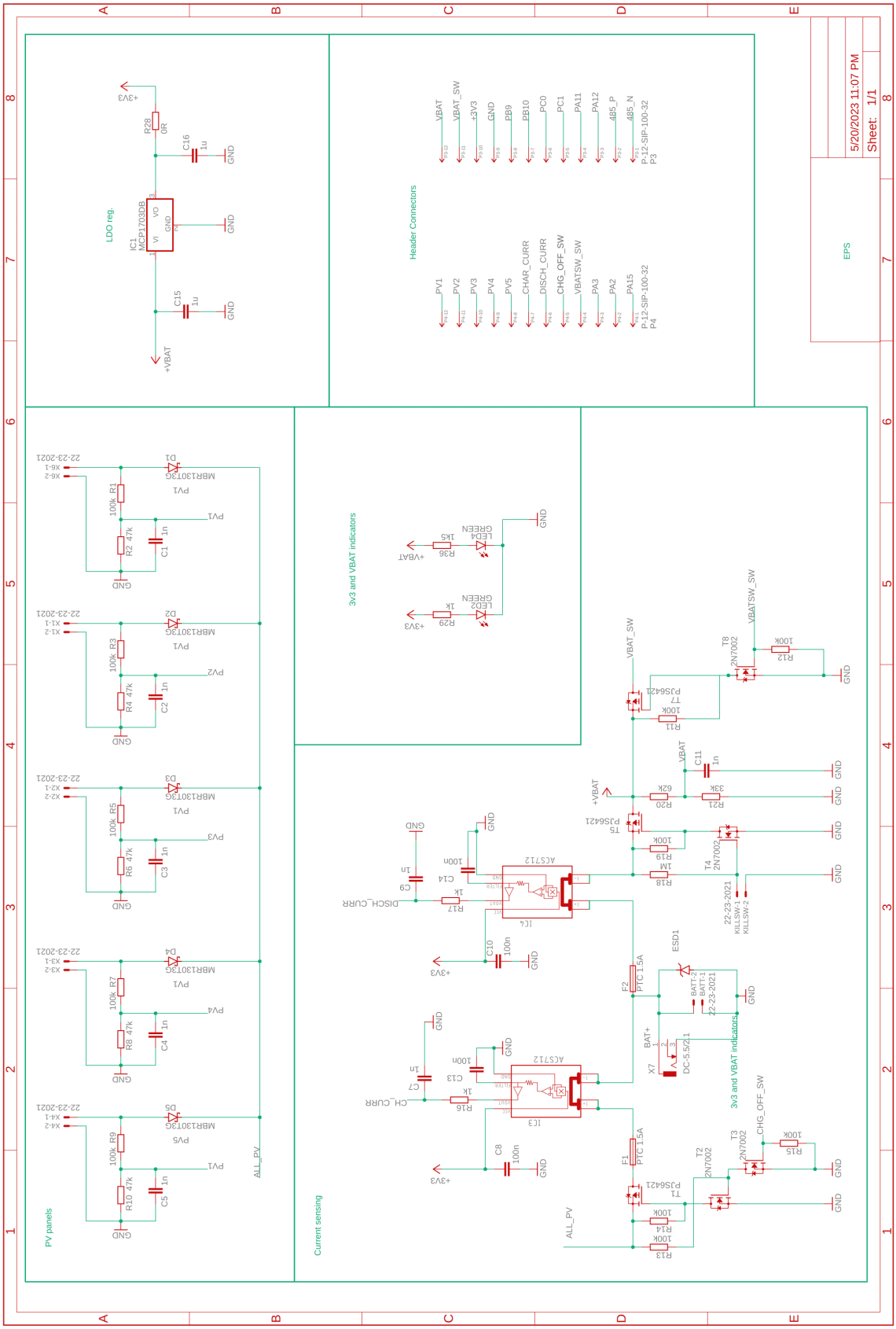

APPENDIX E - OBC+COM PCB (COPPER LAYER)

E1 - TOP SIDE OF PCB – OBC+COM

Scale 1:1 (42mm x 42mm) PCB

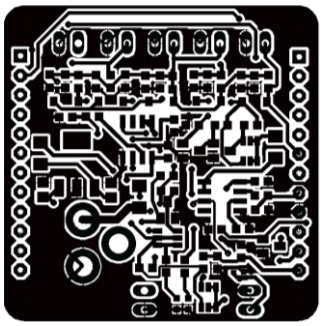

E2 - BOTTOM SIDE OF PCB – OBC+COM

Scale 1:1 (42mm x 42mm) PCB

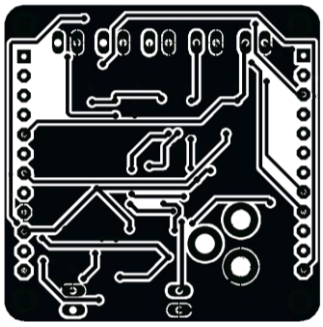

APPENDIX F – COMPONENT PLACEMENT - EPS ()

F1 – COMPONENT PLANECEMENT (TOP)

Scale 2:1

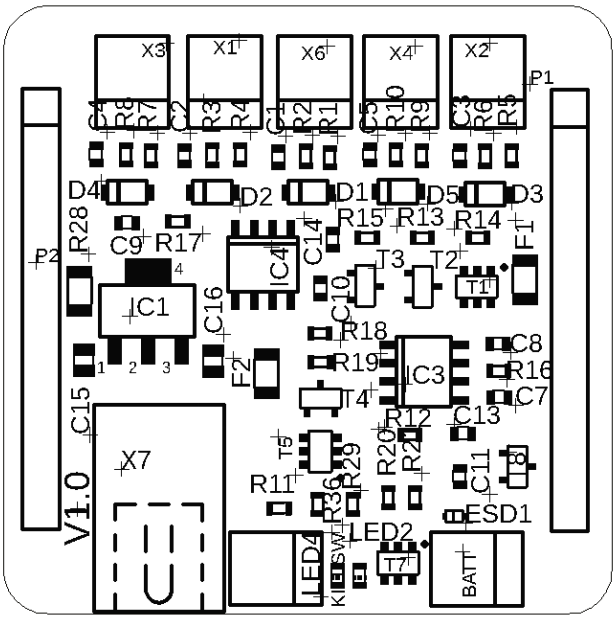

F2 – BOM

Part	Value	Device	Package	Description
BATT	22-23-2021	22-23-2021	22-23-2021	.100 (2.54mm) Center Header - 2 Pin"
C1, C2, C3, C4, C5, C7, C9, C11	1n	C-EUC0603	C0603	Ceramic capacitor
C8, C10, C13, C14, C15, C16	100n	C-EUC0603	C0603	Ceramic capacitor
D1, D2, D3, D4, D5	MBR130T3G	MBR130T3G	SOD123-2	30V, 1A, Schottky diode
ESD1	ESD5Z6.0T5G	ESD5Z6.0T5G	SOD523	6V8 TVS unidirectional diode
F1	PTC 1.5A	FUSE1206	F1206	Fuse
F2	PTC 1.5A	FUSE1206	F1206	Fuse
IC1	LM1117	LM1117	SOT223	0.8A, 16V,LDO Regulator
IC3, IC4	ACS712	ACS712	SO08	Current sensing IC
KILLSW	22-23-2021	22-23-2021	22-23-2021	.100 (2.54mm) Center Header - 2 Pin"
LED2	GREEN	LEDCHIP-LED0603	CHIP-LED0603	LED

LED4	GREEN	LEDCHIP-LED0603	CHIP-LED0603	LED
P1	P-12-SIP-100-32	P-12-SIP-100-32	SIP-100-12-32	HEADER PLUG PINS
P2	P-12-SIP-100-32	P-12-SIP-100-32	SIP-100-12-32	HEADER PLUG PINS
R1, R2, R3, R4, R5, R6, R7, R8, R9, R10, R11, R12, R13, R14, R15	100k	R-EU_R0603	R0603	Resistor
R16, R17	1k	R-EU_R0603	R0603	Resistor
R18	1M	R-EU_R0603	R0603	Resistor
R19	100k	R-EU_R0603	R0603	Resistor
R20	62k	R-EU_R0603	R0603	Resistor
R21	33k	R-EU_R0603	R0603	Resistor
R28	0R	R-EU_R1206	R1206	Resistor
R29	1k	R-EU_R0603	R0603	Resistor
R36	1k5	R-EU_R0603	R0603	Resistor
T1	PJS6421	PJS6421	SOT23-6	20V, 7.4A P-channel MOSFET
T2	2N7002	2N7002	SOT23	2N7002 N-channel MOSFET 60V/210mA,
T3	2N7002	2N7002	SOT23	2N7002 N-channel MOSFET 60V/210mA,
T4	2N7002	2N7002	SOT23	2N7002 N-channel MOSFET 60V/210mA
T5	PJS6421	PJS6421	SOT23-6	20V, 7.4A P-channel MOSFET
T7	PJS6421	PJS6421	SOT23-6	20V, 7.4A P-channel MOSFET
T8	2N7002	2N7002	SOT23	2N7002 N-channel MOSFET 60V/210mA,
X1	22-23-2021	22-23-2021	22-23-2021	.100 (2.54mm) Center Header - 2 Pin"
X2	22-23-2021	22-23-2021	22-23-2021	.100 (2.54mm) Center Header - 2 Pin"
X3	22-23-2021	22-23-2021	22-23-2021	.100 (2.54mm) Center Header - 2 Pin"
X4	22-23-2021	22-23-2021	22-23-2021	.100 (2.54mm) Center Header - 2 Pin"
X6	22-23-2021	22-23-2021	22-23-2021	.100 (2.54mm) Center Header - 2 Pin"
X7	DC-5.5/2.1	DCJ0202	DCJ0202	DC POWER JACK

APPENDIX G- SCHEMATIC OF GROUND STATION

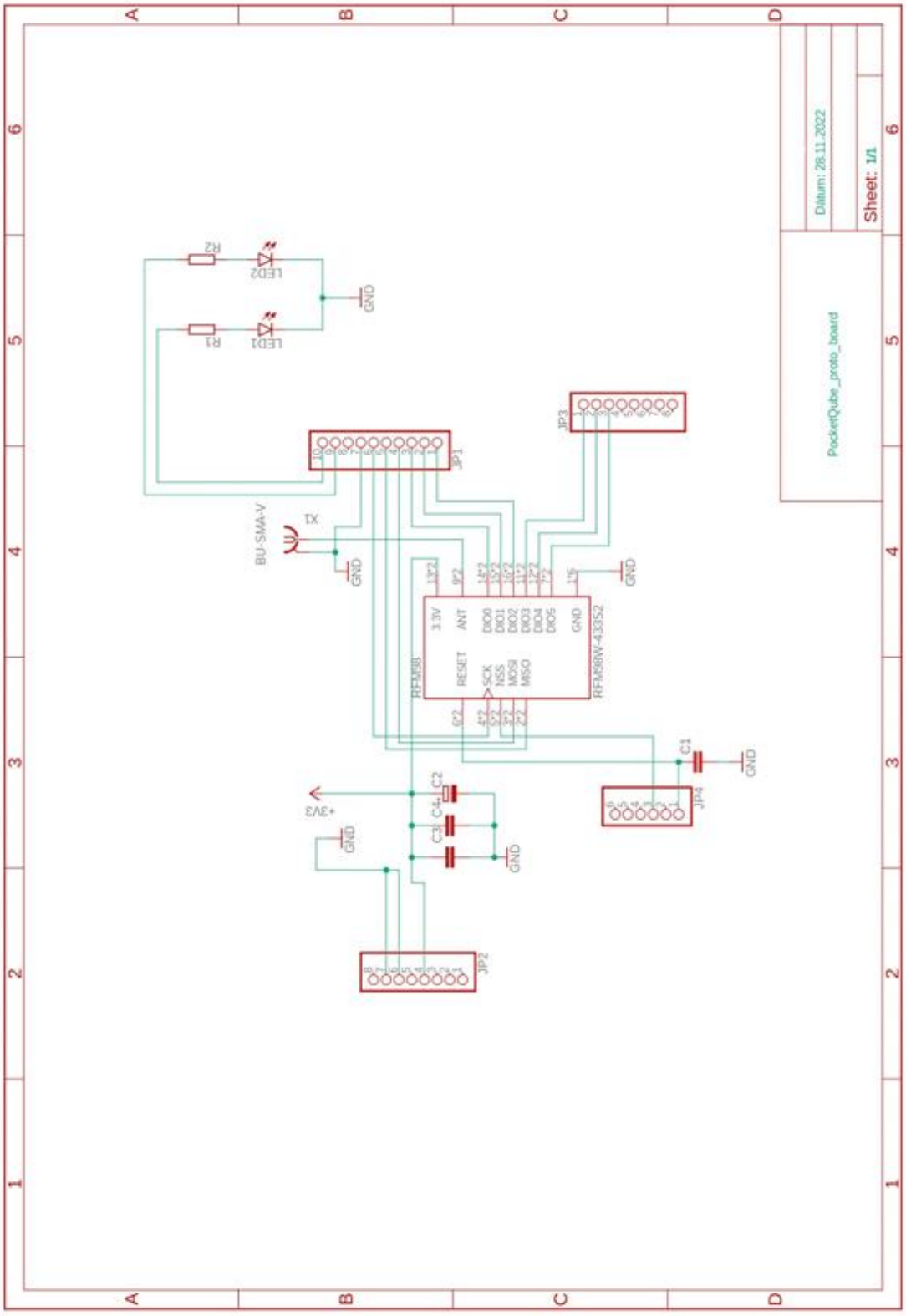

APPENDIX H - GROUND STATION (COPPER LAYER)

H1 - TOP SIDE OF PCB

Scale 1:1

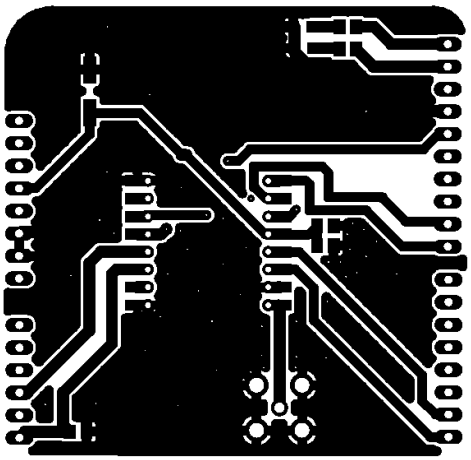

H2 - BOTTOM SIDE OF PCB – OBC+COM

Scale 1:1

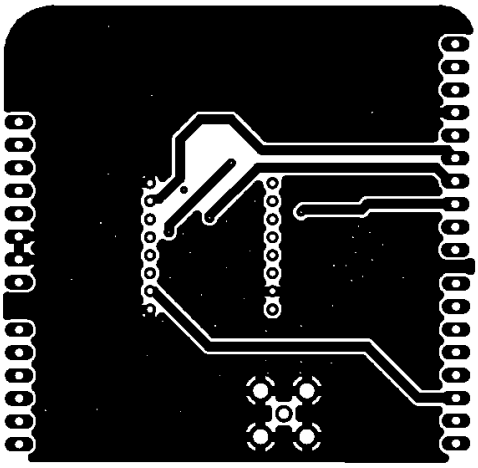

APPENDIX I – COMPONENT PLACEMENT

I1 – COMPONENT PLACEMENT (TOP)

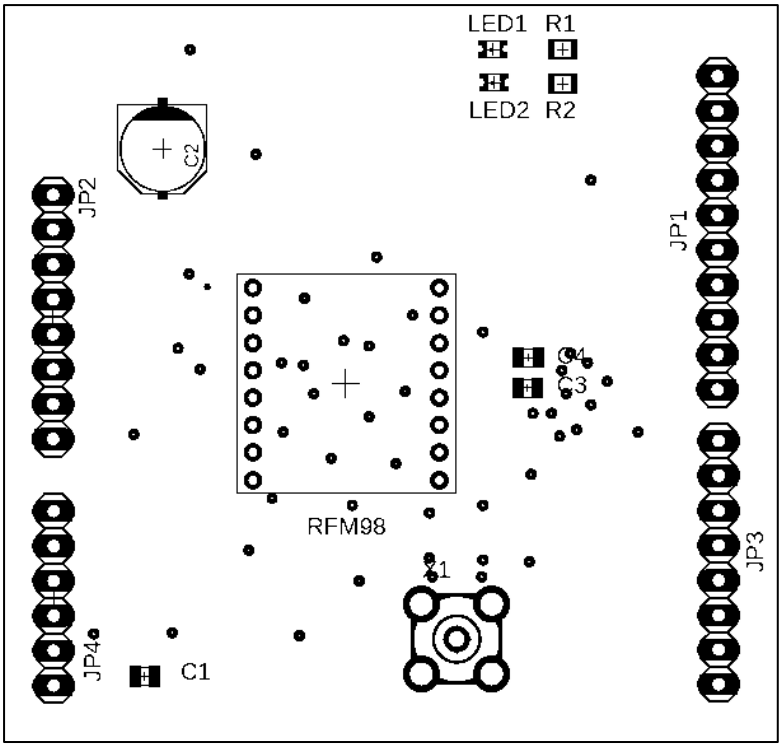

I2 – BOM

Part	Value	Package	Description
C1, C3, C4	100n	C0805	Ceramic condensator SMD
C2	100u	PANASONIC_D	ElectorlyticcondensatorSMD
JP1,JP2,JP3,JP4		1X10	Header 2.54mm
LED1, LED2		CHIPLED_0805	LED diodeSMD
R1,R2	910R	M0805	Resistor SMD
RFM98	RFM98W-433	XCVR	RFM98W
X1	BU-SMA-V	BU-SMA-V	SMA connector

10. APPENDIX J – TECHNICAL DRAWING OF 3D PRINTED FRAME

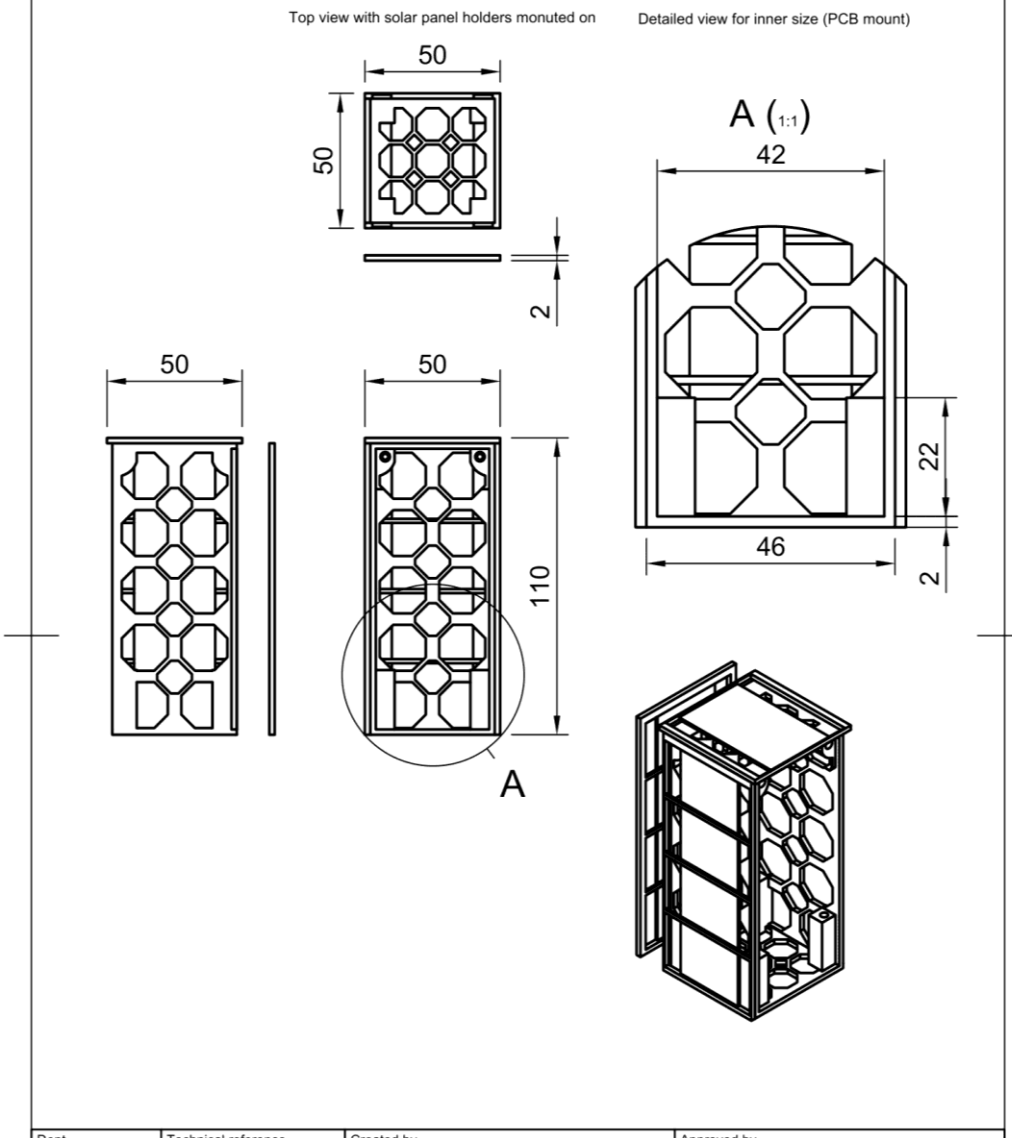

Dept.	Technical reference	Created by	Approved by
		Document type	Document status
		Title: Main frame - PQ1	DWG No.: 2
			Rev. / Date of issue: 5/10/2023 / Sheet: 1/1